

University of Montana

ScholarWorks at University of Montana

Graduate Student Theses, Dissertations, &
Professional Papers

Graduate School

2022

COMBINATORIAL ADMINISTRATION OF SYNTHETIC TLR4 AGONIST INI-2002 AND NOVEL MINCLE AGONIST UM-1098 DELIVERED VIA A-SNPS RESULTS IN SYNERGISTIC IL-1 β PRODUCTION IN HUMAN PRIMARY CELLS AND ENHANCES TH1 AND TH17 RESPONSES IN VIVO

Grace D. Jones

University of Montana, Missoula

Asia Marie Stephanie Riel

University of Montana - Missoula


Alexander Riffey

University of Montana, Missoula

Cassandra Buhl

Follow this and additional works at: <https://scholarworks.umt.edu/etd>

University of Montana, Missoula

 Part of the Immunoprophylaxis and Therapy Commons

Let us know how access to this document benefits you.

Recommended Citation

Jones, Grace D.; Riel, Asia Marie Stephanie; Riffey, Alexander; and Buhl, Cassandra, "COMBINATORIAL ADMINISTRATION OF SYNTHETIC TLR4 AGONIST INI-2002 AND NOVEL MINCLE AGONIST UM-1098 DELIVERED VIA A-SNPS RESULTS IN SYNERGISTIC IL-1 β PRODUCTION IN HUMAN PRIMARY CELLS AND ENHANCES TH1 AND TH17 RESPONSES IN VIVO" (2022). *Graduate Student Theses, Dissertations, & Professional Papers*. 11994.

<https://scholarworks.umt.edu/etd/11994>

This Thesis is brought to you for free and open access by the Graduate School at ScholarWorks at University of Montana. It has been accepted for inclusion in Graduate Student Theses, Dissertations, & Professional Papers by an authorized administrator of ScholarWorks at University of Montana. For more information, please contact scholarworks@mso.umt.edu.

COMBINATORIAL ADMINISTRATION OF SYNTHETIC TLR4 AGONIST INI-2002
AND NOVEL MINCLE AGONIST UM-1098 DELIVERED VIA A-SNPS RESULTS
IN SYNERGISTIC IL-1 β PRODUCTION IN HUMAN PRIMARY CELLS AND
ENHANCES TH1 AND TH17 RESPONSES *IN VIVO*

By

GRACE DAWN MARIE JONES

B.S. Cellular and Molecular Biology, University of Maine, Orono, Maine, 2019

Thesis

presented in partial fulfillment of the requirements
for the degree of

Master of Science

in Cellular, Molecular, and Microbial Biology

University of Montana

Missoula, MT

August 2022

Approved by:

Ashby Kinch, Dean of The Graduate School

Jay T. Evans, Chair

Department of Biomedical and Pharmaceutical Sciences

Scott Wetzel

Division of Biological Sciences

Mike Minnick

Division of Biological Sciences

Erica Woodahl

Department of Biomedical and Pharmaceutical Sciences

Andrij Holian

Department of Biomedical and Pharmaceutical Sciences

Combinatorial Administration of Synthetic TLR4 agonist INI-2002 and Novel Mincle Agonist UM-1098 Delivered via A-SNPs Results in Synergistic IL-1 β Production in Human Primary Cells and Enhances Th1 and Th17 Responses *In Vivo*.

Chairperson: Jay T. Evans

Tuberculosis (TB) kills more people each year than any infectious disease worldwide with recent exception of SARS-CoV-2. Though the Bacille Calmette Guerin (BCG) vaccine confers protection against severe extrapulmonary forms of TB, there is no licensed vaccine for the prevention of pulmonary tuberculosis. The strongest correlate of protection against pulmonary tuberculosis is Th1/Th17 biased cell mediated immunity. Several candidates for TB vaccine adjuvants have shown Th1/Th17 polarizing capacity in clinical trials including Mincle agonist trehalose dibehenate (TDB) and TLR4 agonist monophosphoryl lipid A (MPL). Furthermore, combinatorial administration of MPL and TDB formulated in dimethyldioctadecylammonium (DDA) liposomes has been previously reported to produce synergistic Th1/Th17 immunity. Though this novel combination offered proof of concept for TLR4 and Mincle combination vaccines, use of shorter chain length agonists would afford increased stability and decreased toxicity while maintaining or improving efficacy. Coating of Mincle ligands to silica nanoparticles (SNPs) provides an additional opportunity to form multiple ligand-receptor interactions for increased signaling as previously characterized in Dectin-1. Herein, we characterize several molar ratios of synthetic MPL mimetic INI-2002 and novel TDB derivative UM-1098 delivered via A-SNPs, reporting synergistic IL-1 β production in human peripheral blood mononuclear cells and an increased percentage of CD4⁺ T cells producing Th1/17 cytokines including TNF- α , IL-17, and IFN- γ following combination vaccination against recombinant TB antigen M72.

TABLE OF CONTENTS

CHAPTER 1: INTRODUCTION	1
Tuberculosis As a Worldwide Health Threat	1
Tuberculosis Pathology	2
Clinical Tuberculosis Vaccine Approaches	2
Recombinant Antigens for Subunit Tuberculosis Vaccines.....	4
Table 1: Clinically relevant TB fusion proteins	5
T Cell Activation and Differentiation	6
Table 2: CD4+ T Cell Subsets and Their Defining Features.....	7
Figure 1: CD4+ T Cell Activation and Differentiation	8
Innate Immune Receptors and T Cell Polarization	8
Figure 2: APC recognition of pathogen motifs through PRRs directs the production of T cell polarizing cytokines	9
Toll Like Receptor 4 Agonists	9
Figure 3: TLR4 Signaling Pathways.	10
Macrophage Inducible C-Type Lectin Receptor Agonists.....	11
Figure 4: Mincle/MCL Signaling Pathway	12
Toll Like Receptor 4 Crosstalk with Macrophage Inducible C-Type Lectin Receptor	13
Adjuvant Delivery by Silica Nanoparticles.....	14
Thesis Hypothesis and Project Rationale	14
CHAPTER 2: METHODOLOGY	17
Preparation of Compounds.....	17
Preparation of Formulations.....	19
Table 3: Formulation Details.....	20
Isolation of Human PBMCs	21
Analysis of Cytokine Production	21
In Vivo Experiments	22
ELISA for anti-M72 antibody quantification.....	22
Lymphocyte restimulation and cell-mediated immunity analysis.....	23
Statistical Analysis	24
CHAPTER 3: RESULTS.....	25
<i>In Vitro</i> Stimulation of Human PBMCs.....	25

Figure 5: Coating density dependent responses of UM-1098 on A-SNPs	25
Table 4: Effective Concentrations in Human PBMCs.....	26
Figure 6: Innate cytokine production in human PBMCs.....	27
Table 5: Max cytokine output in human PBMCs	28
Figure 7: Constant addition of 1 μ M UM-1098 to INI-2002 dose response in human PBMCs.....	29
Figure 8: Constant addition of 0.01 μ M INI-2002 to UM-1098 dose response in human PBMCs.....	30
Figure 9: Constant addition of 0.05 μ M INI-2002 to UM-1098 dose response in human PBMCs.....	31
<i>In Vivo</i> Vaccination of C57BL/6 Mice Against M72: Humoral Immunity	31
Figure 10: <i>In vivo</i> study schedule and endpoints.....	32
Table 6: <i>In vivo</i> study conditions.....	33
Figure 11: Post-secondary antibody titers	34
Figure 12. Post-tertiary antibody titers	34
<i>In Vivo</i> Vaccination of C57BL/6 Mice Against M72: Cell-Mediated Immunity	35
Figure 13: Representative T Cell Gating Strategy.....	37
Figure 14: Combination vaccination increases percentage of antigen specific CD4+ T Cells Producing Th1 Biasing Cytokines.....	38
Figure 15: Combination Vaccination Increases IL-17 and IFN- γ Recall Upon Splenocyte Restimulation	39
CHAPTER 4: DISCUSSION.....	40
CHAPTER 5: CONCLUSIONS	45
Summary of Findings	45
Future Directions.....	45
BIBLIOGRAPHY.....	47

CHAPTER 1: INTRODUCTION

Tuberculosis As a Worldwide Health Threat

Tuberculosis (TB) has long remained a leading cause of death worldwide. Apart from SARS-CoV-2, TB kills more people annually than any other communicable disease, exceeding even human immunodeficiency virus (HIV). There were an estimated 1.5 million deaths globally due to tuberculosis in 2021. This estimate by the World Health Organization (WHO) exceeds those of previous years due largely to disruptions in healthcare by the SARS-CoV-2 epidemic (1). The full impact of SARS-CoV-2 related disruptions is yet to be seen; decreased diagnosis and treatment of new and existing infections as well as decreased rates of childhood vaccination during the pandemic threaten global progress against TB. The poor management of tuberculosis during the pandemic has demonstrated that the existing infrastructure and funding for tuberculosis prevention and treatment is unreliable under strain and makes a strong argument for the necessity of an effective vaccine.

The development of rifampicin-resistant TB (RR-TB) and multi-drug resistant TB (MDR-TB) has further stressed the importance of proactive measures against TB. A once curable disease, drug resistance has reduced the efficacy of antitubercular regimens; success rates of treatment in MDR-TB and RR-TB cohorts was estimated at 59% in 2018, an improvement from a previous estimate of 50% in 2012 (1). An estimated 5.7% of all TB cases are diagnosed as drug resistant, though incidence of MDR-TB is disproportionately high in Russia where rates of MDR-TB are estimated at up to 18% of cases (2). The lengthy treatment of MDR-TB requires significant resources and exacerbates

the heavy economic burden caused by TB, already exceeding 1% of total GDP in several high burden countries (3).

Tuberculosis Pathology

The causative agent of TB, *Mycobacterium tuberculosis (Mtb)*, is an acid-fast bacterium transmitted through the inhalation of aerosolized droplets. Disease progression is characterized by a primary infection, latent phase, and a deadly secondary infection also called active TB (4). It's estimated that one tenth of all infected individuals will develop active TB (5). Pulmonary tuberculosis accounts for over 70% of all TB incidence; primary infection in the lung is characterized by the phagocytosis of inhaled bacilli by alveolar macrophages, followed by lysosomal escape and intracellular proliferation (6,7). Recruitment of immune cells to surround the infected macrophages results in granuloma formation which both prevents the dissemination of infection and creates an immune privileged site for the bacteria, allowing for latent infections to persist for decades (6). Active infection is achieved when the granuloma's immune environment is disrupted leading to tissue necrosis and eventual cavitation, freeing the bacteria into the lung and facilitating spread (6). Extrapulmonary TB can have diverse presentations and most commonly manifests in the skeletal system, lymph nodes, pleura, and meninges (8). Extrapulmonary forms of TB were estimated to make up 18% of all new and relapse cases globally in 2020 (1).

Clinical Tuberculosis Vaccine Approaches

The only licensed vaccine for prevention of TB is the Bacille-Calmette Guerin (BCG) vaccine. BCG is composed of live attenuated *Mycobacterium bovis*, a relative of *Mtb*, that infects the host and provokes Th1 immunity (9). Vaccination of infants with BCG

is strongly encouraged to prevent dangerous forms of extrapulmonary tuberculosis such as tubercular meningitis, however BCG isn't protective against pulmonary forms of tuberculosis and is no longer recommended in adults (1,10). Present research aims to develop a vaccine for the prevention of pulmonary tuberculosis.

Among whole cell TB vaccine approaches are those which aim to supplement or improve the present BCG vaccine. Recombinant BCG vaccine VPM1002 demonstrated in clinical trials that, through genetic modification, BCG's efficacy and safety profiles can be improved (11). Others have shown preclinical success in supplementing the BCG vaccine in a prime-boost approach utilizing live attenuated *Mtb* vaccine MTBVAC (12). These whole cell approaches offer advantages including strong immunogenicity and long lasting immunity, however some drawbacks include higher risk of adverse reactions and decreased stability (13,14). Improved safety profiles have made acellular vaccines more attractive to patients over their cellular counterparts. The acellular pertussis vaccine was developed as a reaction to public dissatisfaction with the adverse reactions associated with the whole cell vaccine (14).

Acellular subunit vaccines offer superior safety and ease of mass production in comparison to their whole cell counterparts (13,14). By using only antigens capable of producing protective immunity against a pathogen, subunit vaccines are able to limit off-target effects as well as provoke tailored antigen-specific responses (13,14). Thoughtfully designed recombinant TB antigens can even combine multiple immunodominant epitopes into one protein; recombinant antigens Ag85B-ESAT-6 and M72 are two which have shown promising results in clinical trials (15,16). Adjuvants are necessary additions to subunit vaccines for immunogenicity comparable to that conferred by the naturally

occurring pathogen associated molecular patterns (PAMPs) found in whole cell vaccines. Adjuvants also offer a unique opportunity to direct immune bias by activating pattern recognition receptors (PRRs) with desired downstream effects.

Understanding the correlates of protection against tuberculosis is where rational adjuvant design begins. The strongest correlates for protective immunity against pulmonary TB are T helper type 1 (Th1) and T helper type 17 (Th17) responses (17). Cytokines including interferon gamma (IFN- γ), tumor necrosis factor alpha (TNF- α), interleukin 17 (IL-17), and interleukin 2 (IL-2) are canonical cytokines for protection against TB (18). Adjuvants investigated in TB vaccine clinical trials include toll-like receptor 4 (TLR4) agonist GLA-SE, the two part liposomal adjuvant system CAF01, and TLR4 agonist monophosphoryl lipid A (MPL) delivered with *Q. saponaria* fraction (QS-21) in combination adjuvant system AS01 (16,19,20). These adjuvants have a common goal of biasing the Th1/Th17 responses associated with strong cell-mediated immunity and protection against pulmonary TB.

Recombinant Antigens for Subunit Tuberculosis Vaccines

Mtb expresses some 4000 proteins, many of which are expressed differentially throughout the course of infection (17). This diversity poses significant challenge in the selection of antigen for a subunit *Mtb* vaccine. Proteomic analysis of *Mtb* lysates among infected individuals yield the most valuable insights into antigens which differentiate latent and active *Mtb* infections (17,21). Systematic exposure of antigens to peripheral blood mononuclear cells (PBMCs) sourced from *Mtb* infected individuals and subsequent immunological assessment by T cell proliferative assays as well as interferon release assays have allowed identification of which *Mtb* proteins have putative T cell epitopes capable of

provoking strong cell mediated immunity *in vivo* (22). Recombinant technologies afford the opportunity to select multiple epitopes and join them into a singular fusion protein, thereby accounting for heterogenous protein expression throughout infection. Several such recombinant *Mtb* antigens have progressed to clinical trials for use in both TB preventatives and therapeutics including H1, H4, H56, ID93, CysVac2, and M72 (23,24). These fusion protein components and their clinically tested applications are detailed in Table 1.

Fusion Protein	Antigens	Vaccine Formulations
H56	Ag85B ESAT6 RV2660	H56:IC31
		H56/CAF01
		H56+K31
M72	Mtb39a Mtb32a	M72/AS01E
H1	Ag85B ESAT6	H1:IC31
		H1:CAF01
ID93	Rv1813 Rv2608 Rv3619 Rv3620	ID93+GLA-SE
CysVac2	Ag85B CysD	CysVac2/Advax™
H4	Ag85B TB10.4	H4:IC31 (AERAS-404)

Table 1: Clinically relevant TB fusion proteins

Though no work has been done to directly compare candidate fusion antigens, a cross-study comparison of clinically evaluated *Mtb* vaccines analyzed efficacy across eight in-human clinical trials as determined by antigen specific T cell memory responses. Treatments investigated included the subunit vaccines H56:IC31, M72:AS01E, H1:IC31, and ID93: GLA-SE, the viral vector vaccines AERAS-402 and MVA85A, as well as the clinically licensed live-attenuated BCG. This comparison showed that while all clinical candidates induced Th1 but not Th17 biased immunity, M72/AS01E cohorts showed the

most potent production of T cell memory (23). These data conclusively show that M72 as a recombinant *Mtb* antigen is capable of provoking strong cell-mediated immunity *in vivo*. The work detailed herein utilizes M72 fusion protein as a model antigen for the comparison of T cell responses elicited by several adjuvant formulations *in vivo*.

T Cell Activation and Differentiation

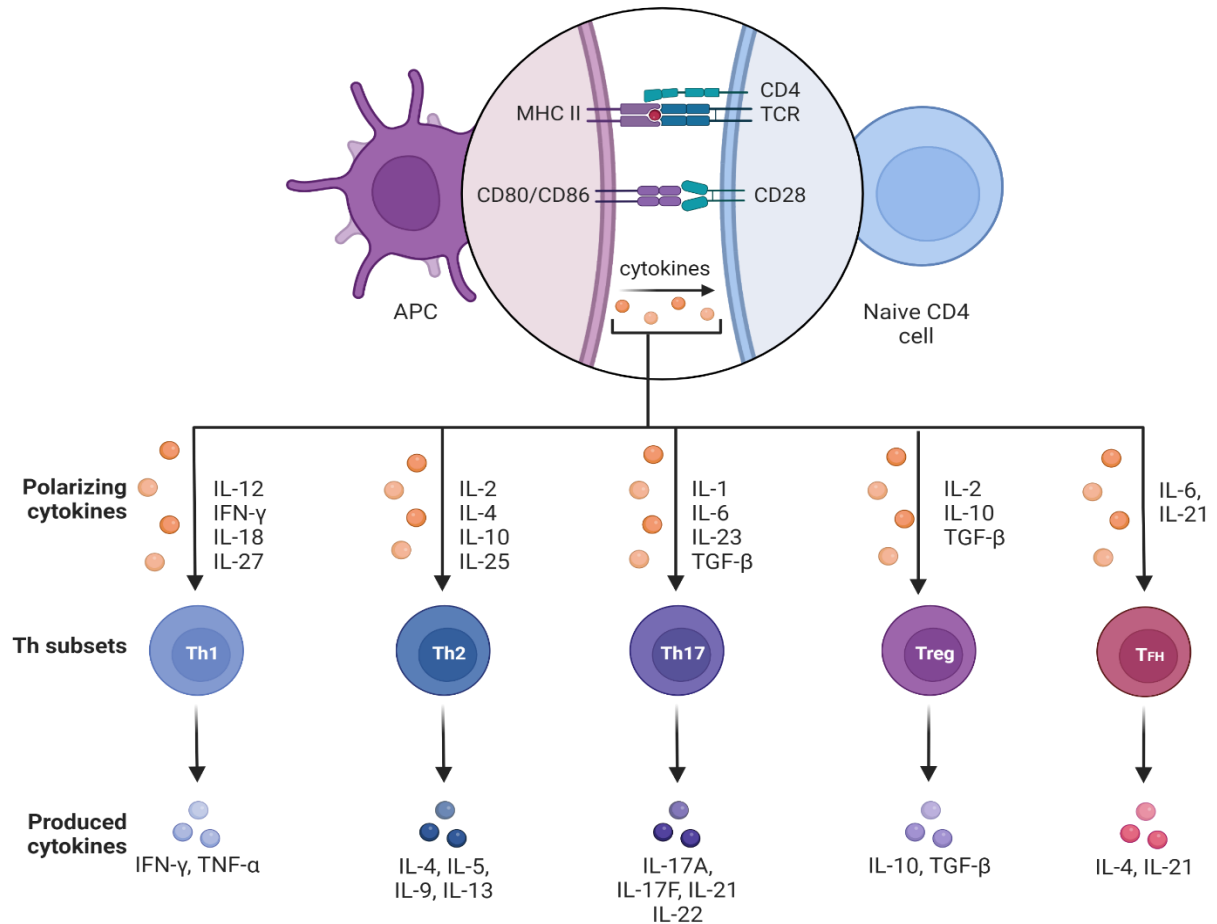
T cells are adaptive immune cells which recognize antigens and are divided into those which perform cytotoxic functions and those which perform immunomodulatory functions (25). These two subsets can be distinguished by their cell surface markers CD8 and CD4, respectively. CD8-positive cytotoxic T lymphocytes (CTLs) recognize intracellularly derived antigens presented through major histocompatibility complex I (MHC I) to distinguish healthy cells from those infected with intracellular pathogens or cancerous cells (26). CTLs direct the presenting cell to undergo apoptosis if the proteins presented aren't recognized as normal self-antigens, thereby limiting spread of infection. CD4-positive T helper cells are further divided into subsets defined by their effector cytokines and functions, and include regulatory T cells (Tregs), Th17, Th1, Th2, and T follicular helper cells (T_{FH}) (26). The many subsets of T helper cells are a direct reflection of the diversity of pathogens they combat; the resulting toolkit allows for specialized immunity against each type of threat. Table 2 summarizes the functions of major CD4 T cell subsets and their indicators.

Subset	Polarizing Cytokines	Transcription Factor	Effector Cytokines	Effector Functions
T Reg	IL-2, IL-10, TGF- β	FOXP3	IL-10, TGF- β	Regulation and dampening of immune responses
Th1	IL-12, IFN- γ , IL-18, IL-27	T-Bet	IFN- γ , TNF- α	Intracellular immunity, CTL and macrophage activation, inflammation
Th2	IL-2, IL-4, IL-10, IL-25	GATA3	IL-4, IL-5, IL-9, IL-13	Extracellular immunity, antibody production, allergy
Th17	IL-1, IL-6, IL-23, TGF- β	ROR γ t	IL-17A, IL17F, IL-21, IL-22	Inflammation, intracellular immunity
T_{FH}	IL-6, IL-21	Bcl-6	IL-4, IL-21	B cell help, antibody class switching

Table 2: CD4⁺ T Cell Subsets and Their Defining Features

Naïve CD4⁺ T cells differentiate into the appropriate subtype during T cell activation by antigen presenting cells (APCs). APCs are responsible for phagocytosis and digestion of foreign bodies, and then presentation of foreign peptides to T cells for the development of adaptive immunity (26). Naïve CD4⁺ T cells must recognize antigen presented on major histocompatibility complex II (MHC II) as well as receive an activating signal through CD28 to become mature antigen-specific effector cells (25). Cytokines released by the APC during activation direct the T cell to commit to a master transcription factor which will ultimately determine its effector subset. Figure 1 depicts antigen recognition, co-stimulation of CD28, as well as the delineation of subsets based on the polarizing cytokines released into the immune milieu during activation. CD4⁺ subsets are defined for ease of explanation, although cells can express properties of multiple subsets simultaneously and are not committed to a subset for life.

Figure 1: CD4+ T Cell Activation and Differentiation. Figure created in Biorender.

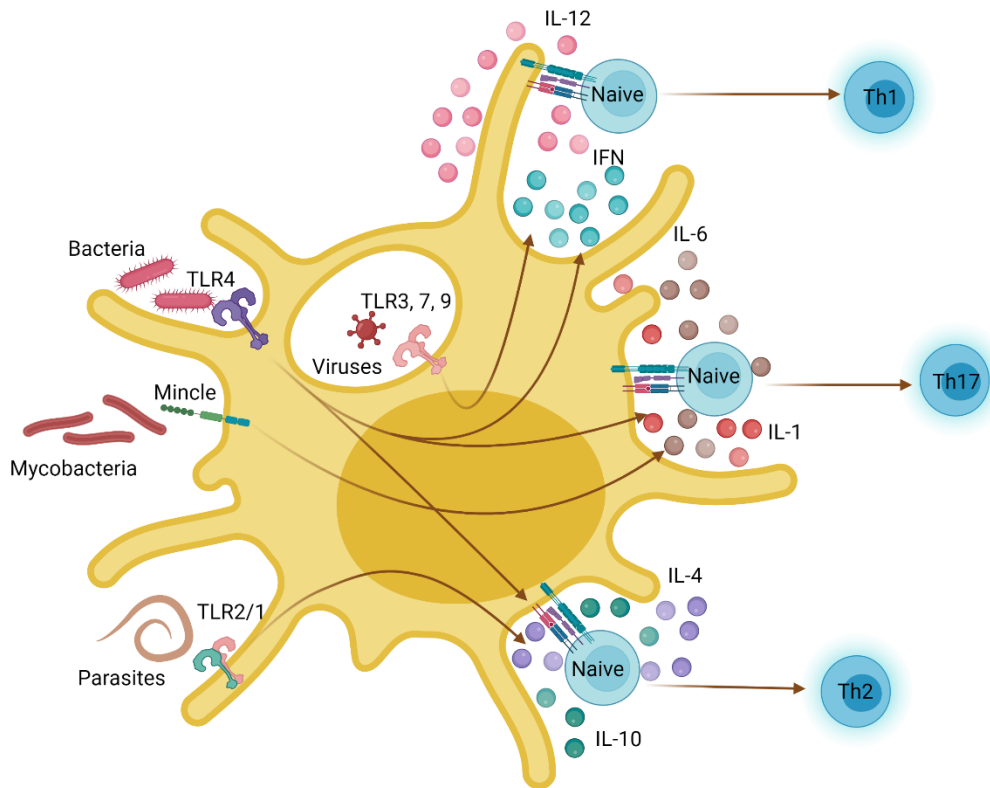


Innate Immune Receptors and T Cell Polarization

The specific cytokines released during antigen presentation are dependent on PAMPs recognized by the APC. PAMPs are motifs conserved across genres of pathogens that inform innate immune cells of pathogen characteristics including cell wall components or nucleic acid structure. For example, motifs distinct to viruses are recognized through PRRs who's downstream signaling induce cytokines that polarize Th1 biased immunity to eliminate this perceived intracellular threat (26). In this way PRRs can tell T cells not just

what the antigen looks like, but also what type of response will be most effective when the antigen is encountered. Figure 2 briefly summarizes recognition of diverse pathogens through PRRs and the downstream release of T cell polarizing cytokines for tailored immune memory.

Figure 2: APC recognition of pathogen motifs through PRRs directs the production of T cell polarizing cytokines. Figure created in BioRender.



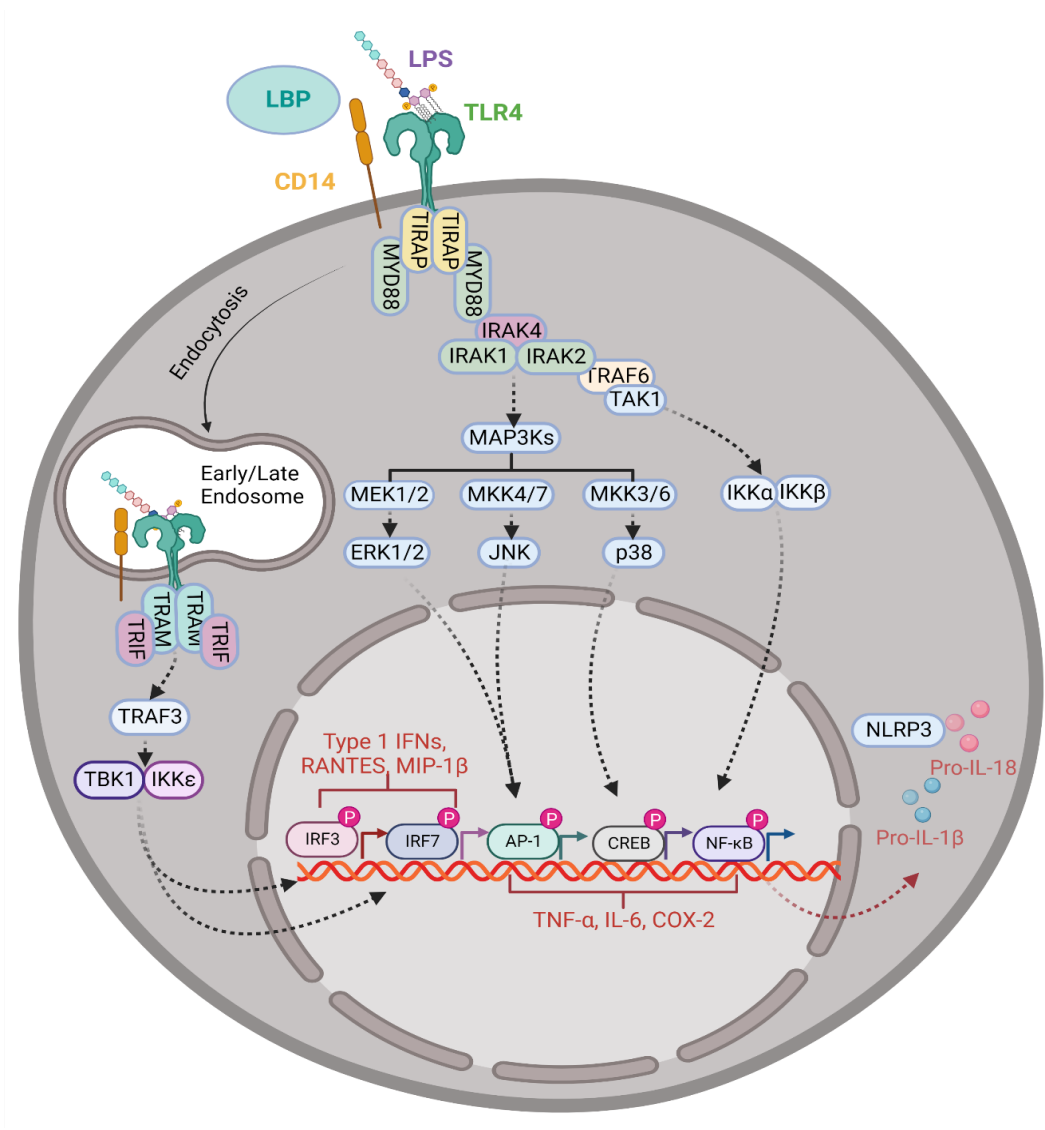
Synthetic agonists targeting PRRs provide a novel opportunity for immune therapeutics and vaccine adjuvants to direct cell-mediated immunity.

Toll Like Receptor 4 Agonists

TLR4 is a type I transmembrane glycolipid responsible for the detection of damage associated molecular patterns and bacterial PAMP lipopolysaccharide (LPS). TLR4 is primarily expressed on the cell surface where it signals through MyD88, although following endocytosis TLR4 is able to signal through TRIF in a MyD88

independent fashion (27). Signaling through MyD88 results in the phosphorylation of transcription factors AP-1, CREB, and NF- κ B, which in turn induce production of pro-inflammatory cytokines as well as inflammasome activators. In contrast, activation through TRIF results in downstream phosphorylation of IRF3 and IRF7 and the production of type I interferons (IFNs) and chemokines (27). Figure 3 summarizes TLR4 signaling pathways and their outputs.

Figure 3: TLR4 Signaling Pathways. Figure created in BioRender.

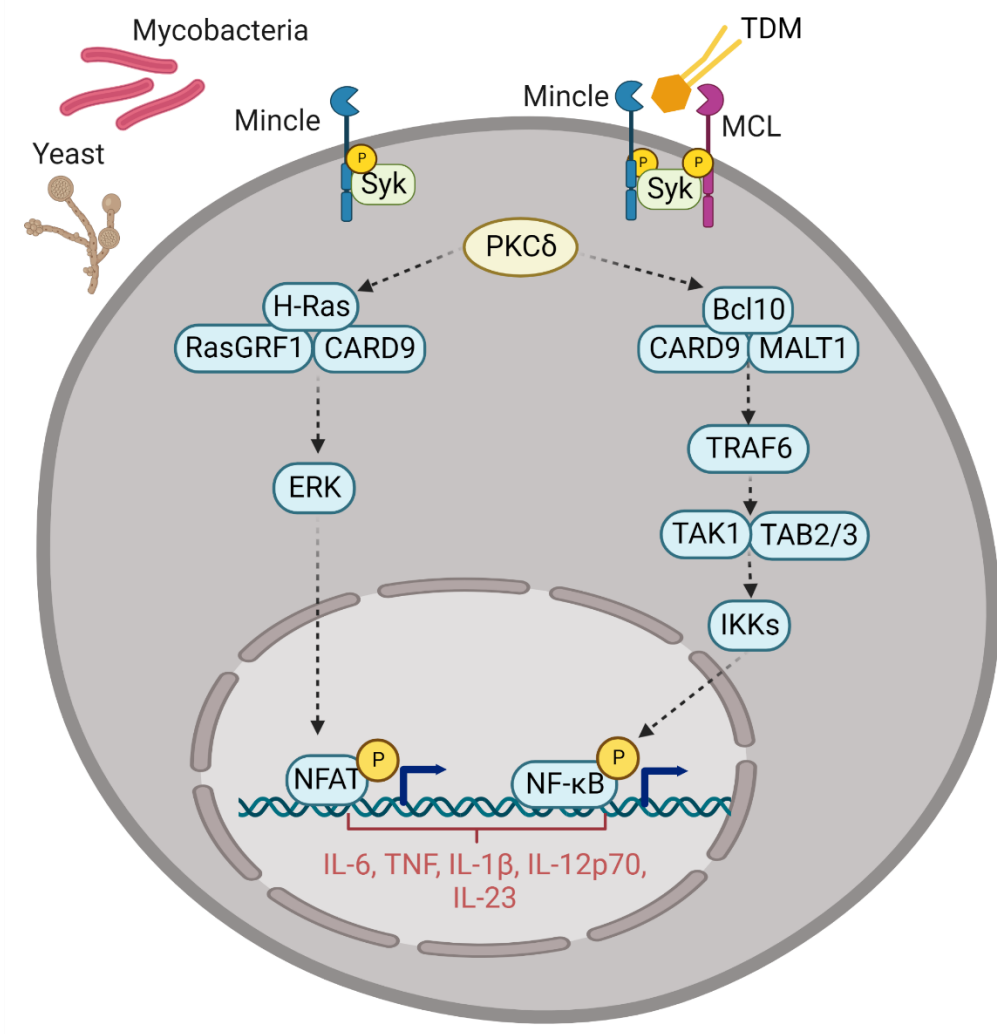


Multiple vaccines adjuvanted with TLR4 agonists have been licensed or reached in-human clinical trials. Adjuvant System 04 (AS04), a two-part system composed of TLR ligand MPL and aluminum salt, skews the immune response towards a Th1 bias with CD4+ T cells producing type I interferons, making it an effective adjuvant against intracellular pathogens (28). Ceravix™ and Fendrix™ use AS04 to target human papillomavirus and hepatitis B respectively, both of which require potent Th1 cell-mediated immunity for protection. Adjuvant System 01 (AS01) similarly induces Th1 biased immunity through immunostimulants MPL and QS-21 in a liposomal formulation, and is under investigation in clinical trials for candidate malaria and is approved for Shingrix™ (29). MPL has been characterized as biasing TRIF signaling, reducing toxicity compared to its parent compound LPS for improved safety (30). Future TLR4 adjuvants may include synthetic lipid A analogs with reduced fatty acid chains that maintain the safety profile of MPL, however offer improvements to its solubility and stability (31). Our lab has previously designed and characterized lipid A mimetics with improved toxicity/efficacy profiles including the compound INI-2002 used herein (32,33).

Macrophage Inducible C-Type Lectin Receptor Agonists

Macrophage inducible C type lectin (Mincle) is a surface PRR present on select APCs responsible for the recognition of mycobacterial cell wall carbohydrates. Mincle can signal alone or as a homodimer with macrophage restricted C type lectin (MCL) with whom it shares many ligands. Mincle/MCL signal through Syk to modulate transcription via NFAT and NF- κ B as illustrated in Figure 4 (34,35). Downstream induction of IL-6, TNF, IL-1 β , IL-12p70, and IL-23 make Mincle a potent mediator of Th1/Th17 polarization, making it an excellent clinical vaccine target.

Figure 4: Mincle/MCL Signaling Pathway. Figure Created in BioRender



Other than the BCG vaccine itself, Freund's Complete Adjuvant (FCA) was the first vaccine or adjuvant system to contain Mincle agonists. A water in oil emulsion with whole-cell killed *Mycobacterium*, CFA induced such potent Th1/Th17 immunity it later became a tool used to induce and study both autoimmunity and chronic pain *in vivo* (36). Mycobacterial cord factor, trehalose 6'6-dimycolate (TDM), was later identified as a mycobacterial PAMP responsible for inducing potent Th1/Th17 responses through Mincle. Synthetic TDM analogs designed for reduced toxicity have since been investigated as candidate Th1/Th17 biasing adjuvants (37). Cationic formulation 01 (CAF01), a

dimethyldioctadecylammonium (DDA) liposome formulated with cord factor analog trehalose 6'6-dibehenate (TDB), has entered clinical trials for safety and efficacy as an adjuvant for chlamydia as well as tuberculosis vaccines (20,38).

CAF01 provides a strong benchmark for future adjuvant design, however TDB's poor solubility and DDA's instability leave room for improvement (39). Our group has previously reported on the structure activity relationship of several classes of synthetic trehalose analogs for the discovery of safe, effective, and easily formulated Th17 biasing agonists (40,41). This work will detail the use of a novel unpublished synthetic trehalose derivative UM-1098 selected based on inducing Th17 mediated immune responses delivered in a stable silica nanoparticle (SNP) formulation.

Toll Like Receptor 4 Crosstalk with Macrophage Inducible C-Type Lectin Receptor

Scientists first discovered Mincle when the stimulation of macrophages with TLR4 ligand LPS induced transcription of its encoding gene *Clec4e* (42). Mincle has since been characterized as minimally expressed unless induced by LPS, TNF- α , IL-6, or IFN- γ (43). Mincle on the contrary is associated with the suppression of TLR4 signaling through downregulation of co-receptor CD14 and thereby functions to limit TLR4 induced toxic shock. (42,44). In this way Mincle and TLR4 provide checks and balances in innate immune responses.

A novel DDA liposomal formulation combining MPL and TDB (DMT) has demonstrated proof of concept for combination Mincle and TLR4 adjuvant systems (45,46). DMT adjuvanted subunit vaccines were able to confer protection equal to or greater than that of BCG as measured in TB challenge with H37Rv strain (46). Importantly, DMT protected against reactivation of latent TB (46). DMT produced higher levels of IFN-

γ , IL-2, TNF- α , and IL-17A when compared with DDA-TDB and DDA-MPL formulations, demonstrating the synergy between TDB and MPL components (45).

It should be noted that combination adjuvants are not limited to uses in vaccines. Combination of ultra-pure LPS and TDB was recently noted to aid in restricting *Mtb* infection when applied with isoniazid or rifampicin by means of induced autophagy (47). Coadministration of adjuvants with antitubercular treatment not only enables dose sparing of antibiotics, but also provides a novel approach to combatting drug resistant TB.

Adjuvant Delivery by Silica Nanoparticles

Delivery systems offer several advantages to therapeutics including stabilization of conformation, prolonged antigen exposure, codelivery of antigen and adjuvant, as well as potential for complex formation with multiple ligands (48,49). Dectin-1, a member of the family of C type lectin receptors (CLRs), has demonstrated that binding of multiple receptors is necessary for potent downstream signaling, suggesting that controlled coating density on delivery vehicles could aid in complex formation and signaling in the CLR family (50). Indeed, in the work detailed here we note that coating-density of Mincle agonist UM-1098 on aminopropyl-SNPs (A-SNPs) drastically impacts immunogenicity in a species-specific fashion.

Thesis Hypothesis and Project Rationale

Cell-mediated immunity is necessary for protection against intracellular pathogens including the worldwide health threat tuberculosis, particularly Th1 and Th17 responses. Both TLR4 and Mincle agonists have demonstrated their value in clinical trials as adjuvants provoking Th1/Th17 cell-mediated immunity. Combination of TLR4 agonists (MPL or ultra-pure LPS) and TDB has been demonstrated to provoke greater immunogenicity than

either agonist alone both in DDA based vaccines as well as in therapeutics. We have aimed to reform this design through use of synthetic agonists with shorter lipid chains to both increase solubility and decrease toxicity. TLR4 agonist INI-2002 and Mincle agonist UM-1098 were selected for combination based on their induction of potent Th17 biased immunity.

In lieu of DDA liposomes we have chosen to pursue SNPs as a rational delivery mechanism with greater stability and feasibility in resource poor areas. The decision to use SNPs was partially founded on the hypothesis that coating Mincle agonists onto SNPs affords an opportunity to form multiple PRR-ligand complexes as previously demonstrated with Dectin-1, with higher coating densities allowing for stronger signaling through Mincle. To ensure that UM-1098 could form multiple complexes on a single cell, agonists were adsorbed to silica independently and admixed.

Several molar ratios were investigated for the coadministration of UM-1098 and INI-2002 in order to find where additive/synergistic responses occur as well as where they were ablated. Given that both receptors are responsible for regulating each other's expression and signaling, we hypothesized finding an inflection point where negative feedback would reduce innate cytokine production *in vitro* and thus decrease downstream Th1/Th17 cell-mediated immunity. Based on previous *in vivo* dose selection data suggesting that 50nmol/mouse and 1nmol/mouse doses were optimal for UM-1098 and INI-2002 respectively, a 50 to 1 molar ratio was chosen as a logical starting point. The overall hypothesis was that synergy would be observed at the molar ratio reflective of each API's optimal dose regimen, whereas straying from this molar ratio in either direction

would diminish or eliminate synergy. The final selection of ratios for *in vitro* screening ranged between 500:1 and 5:1 (UM-1098:INI-2002).

Indicators of innate synergy were chosen based on innate cytokines induced by each PRR including IL-1 β , TNF- α , and IL-6 being shared by both PRRs while RANTES was chosen to distinguish the TRIF pathway of TLR4. Murine T cell responses following vaccination were chosen as the main readout of adaptive synergy, with assessment of intracellular cytokine production upon antigen restimulation as measured by flow cytometry heavily prioritized, with IL-17 and IFN anticipated as primary synergistic adaptive cytokines. This thesis was originally intended to include data following *Mtb* challenge in mice vaccinated with a lead combination formulation, however the challenge study was ongoing at the time of thesis submission and will be discussed in the future directions section.

CHAPTER 2: METHODOLOGY

Preparation of Compounds

INI-2002 was synthesized as previously described at Inimmune Corp. (32). UM-1098 was synthesized by the Center for Translational Medicine medicinal chemistry team at the University of Montana; and Asia Riel's, Ph.D. write up on the synthesis of UM-1098 is detailed as follows. Reactions were monitored by TLC-analysis on Merck Silica gel 60 F254 plates and visualized by UV at 254 nm and dipping in vanillin (vanillin/water/ethanol/sulfuric acid, 0.2 g:5 mL:5 mL:1 mL) or phosphomolybdic acid in ethanol (PMA) and developed with heat. Compounds were confirmed to be >95% pure by NMR and HPLC-CAD analysis. ^1H and ^{13}C NMR spectra were recorded on an Agilent or Bruker 400 MHz instrument and were referenced to TMS or a solvent peak. High-resolution HPLC-MS analysis was obtained on an Agilent 6520 Q-TOF mass spectrometer utilizing an electrospray ionization source in positive or negative mode. Chromatography was performed on Grace or Biotage automated medium pressure chromatography instruments with preloaded Buchi silica gel cartridges. 2,2',3,3',4,4'-Hexa-*O*-benzoyl- α,α -D-trehalose and 2,2',3,3',4,4'-Hexa-*O*-benzoyl-6,6'-bis(methanesulfonyl)- α,α -D-trehalose were prepared using the literature method without any modification (51).

BSA (140mL), followed by TBAF (4mL, 0.04 mmol) was added dropwise to a solution of α,α -D-trehalose dihydrate (25 g, 66 mmol) in dry DMF (100 mL). The reaction mixture was stirred for 1 hr and then quenched with 2-propanol (25 mL). Reaction mixture was frozen to -20 °C for 1 hr and then treated with a cooled solution of K_2CO_3 (9.1 g, 66 mmol) in 2000 mL of MeOH. After stirring for 10 min, the solution was neutralized with acetic acid and then methanol was removed *in vacuo*. The resulting residue was extracted

with heptane and then the organic layer washed with brine and concentrated *in vacuo* to produce a crude product. The purification of crude product was carried out by column chromatography. **¹H NMR (400 MHz, DMSO-d₆)** δ 4.82 (d, *J* = 2.93 Hz, 1H), 4.58 (s, 1H), 3.81 - 3.89 (m, 1H), 3.69 (d, *J* = 10.51 Hz, 1H), 3.50 (d, *J* = 8.93 Hz, 2H), 3.40 (dd, *J* = 3.06, 9.17 Hz, 1H), 3.33 (s, 1H), 0.03 - 0.16 (m, 27H); **¹³C NMR (100 MHz, DMSO-d₆)** 93.5, 73.5, 73.3, 72.4, 71.0, 59.8, 1.1, 0.15.

To a stirred mixture of 2,2',3,3',4,4'-Hexa-trimethylsilyl- α,α -D-trehalose (1 eq.; 1 mmol), aryl carboxylic acid (2.2 eq.; 2.2 mmol) and DMAP (3 eq.; 3 mmol) in anhydrous DCM (10 mL) was added DCC (3 eq.; 3 mmol) or EDCI-MeI (3 eq.; 3 mmol) at 0 °C for 30 min and then at room temperature overnight. The reaction mixture was diluted with water and then extracted with DCM. The combined organic layer was dried over MgSO₄ and reduced *in vacuo*. The crude mixture was subjected to chromatography using the Biotage system with a 12 g silica column and a 0-20% ethyl acetate in heptane gradient. This yielded the silyl intermediate in good to excellent yields.

The silyl intermediate (0.333 mmol) was dissolved in equal amount of methylene chloride and methanol (8 mL) treated with Dowex 50WX8 resin (668.4 mg) with magnetic stirring. Upon consumption of the starting material as determined by TLC (20% methanol in methylene chloride and charring with vanillin stain) the reaction was filtered, concentrated, and chromatographed on a silica column, followed by eluting with a 40-80% methylene chloride to methanol gradient (Biotage system using a 12 g pre-packed column) to provided desired product (63% for coupling and deprotection). **¹H NMR (400 MHz, DMSO-d₆)** δ 7.13 (s, 4H), 5.17 (br, 2H), 4.98 (d, *J* = 8.9 Hz, , 4H), 4.85 (d, *J* = 4.4 Hz, 2H), 4.46 (d, *J* = 9.2 Hz, 2H), 4.14 (br, 2H), 4.04 (br, 2H), 3.84 (br, 12H), 3.64 (br, 2H), 3.28 (br,

2H), 3.16 (br, 2H), 1.60 (br, 12H), 1.33 (br, 12H), 1.16 (br, 48H), 0.76 (br, 18H); ¹³C NMR (100 MHz, DMSO-d₆) 165.17, 152.29, 141.39, 124.48, 107.13, 92.90, 72.71, 72.40, 71.67, 70.62, 69.70, 68.21, 64.48, 31.29, 31.22, 29.79, 28.88, 28.77, 28.76, 28.73, 25.59, 25.52, 22.08, 13.79, 13.76. **HRMS:** C₂₈H₂₈F₆O₁₃ NH₄⁺ requires 1336.9237 Found 1336.9222.

Preparation of Formulations

A-SNPs formulations were prepared by Alexander Riffey in the Burkhart lab at the University of Montana. A-SNPs were first prepared by modifying the surface chemistry of silica nanoparticles (SNPs) purchased from nanoComposix, Inc. (Non-Functionalized NanoXact Silica.) SNPs were washed from Type 1 ultrapure water into anhydrous ethanol (EtOH) via centrifugation, then dried via rotary evaporation at 40°C. Dried SNPs were weighed and transferred into a round bottom flask, where they were resuspended at 10 mg/mL in water for irrigation, USP (WFI) via bath sonication for approximately 30 minutes (37kHz, 20-30°C). The flask was charged with 0.105 μL (3-Aminopropyl) triethoxysilane per mg of SNP and processed via bath sonication for 3 hours (37kHz, 70°C) to modify the silica surface with aminopropyl moieties. After processing, the reaction flask was magnetically stirred overnight at room temperature. ASNPs were recovered by centrifugation and subsequently washed with 5 reaction volumes of WFI followed by 5 reaction volumes of EtOH, then dried via rotary evaporation at 40°C and stored at room temperature.

Stock suspensions of A-SNPs were prepared in EtOH using bath sonication as described for SNPs above. Stock solutions of the agonists UM-1098 and INI-2002 were prepared by vortexing in THF:MeOH (9:1, v/v) and MeOH, respectively. Aliquots of the A-SNP stock suspensions and the agonist stock solutions were transferred quantitatively

into 2 mL round-bottom glass vials and mixed for 10 seconds before drying into a thin film via speedvac vacuum concentrator until the vacuum reading reached approximately 300 mtorr (45°C heating for 1 hr, 2 hr run time, vacuum ramp 3.) After drying, sterile filtered suspension vehicle was added to each sample vial immediately before processing. Sample processing included bath sonication for 1 hr (37kHz, 55-65°C) followed by focused sonication via Covaris S2 for 5 minutes (37°C, 10% duty cycle, intensity 8, 1000 cycles/burst in 15 second treatments for 20 cycles.) Samples were finally stored at 2-8°C for 72 hr before use and characterization. Formulation characterization included DLS particle sizing and zeta potential (Malvern ZEN 3600), sample pH, osmometry (EliTechGroup VAPRO 5600), and total suspended agonist concentration via HPLC (Waters Alliance 2695e with 2998 PDA detector.) Samples were vortexed at 3000rpm for 30 seconds immediately before use.

Formulation Intended Use	API	API Concentration (uM)	A-SNP Size (nm)	SNP Concentration (mg/mL)	Solvent
<i>In vivo/ In vitro</i>	-	-	50	25	2% Glycerol
<i>In vitro</i>	UM-1098	1000	200	10	2% Glycerol
<i>In vivo</i>	UM-1098	2500	50	22	2% Glycerol
<i>In vivo</i>	UM-1098	1000	200	10	2% Glycerol
<i>In vitro</i>	INI-2002	820.5	50	10	WFI
<i>In vivo</i>	INI-2002	50	50	22	2% Glycerol

Table 3: Formulation Details

Prior to use *in vivo*, a stock of each injection condition was made and incubated on a rotating mixer for an hour for adsorption of M72 antigen.

Isolation of Human PBMCs

Peripheral blood samples were collected from healthy adult donors. The samples were collected after approval by the University of Montana Institutional Review Board (43–16) and signed written informed consent was obtained from each donor. Peripheral blood mononuclear cells (PBMC) were isolated from peripheral blood using Ficoll-Paque,. Briefly, heparin-anticoagulated blood was diluted with an equal volume of Dulbecco's phosphate-buffered saline, pH 7.4 (DPBS), and 35 mL of diluted blood was layered over 15 mL of the Ficoll-Paque (Sigma). Gradients were centrifuged at 400×g for 30 min at room temperature in a swinging-bucket rotor without the brake. The PBMC interface was carefully removed by pipetting and washed with PBS-5%FBS followed by centrifugation at 250×g for 10 min. This was followed by a second wash with PBS-5%FBS. Cells were resuspended in RPMI medium with 5% autologous plasma. Cell number and viability were determined using a hemocytometer. Non-viable cells were identified by trypan blue staining and cell counts were calculated on viable cells only. Cells were added at 6x10⁶ cells/well in RPMI with 5% autologous plasma to serially diluted formulations. Supernatants were harvested from treated cells at 24 hr post-cell application.

Analysis of Cytokine Production

Supernatants from human PBMCs were analyzed using either a DuoSet ELISA (R&D Systems, Minneapolis, MN) for human IL-6, TNF- α , IL-1 β , or RANTES, or a multiplex panel for analytes TNF α , IL-1 β , IL-6, IFN- γ , IL-12p70 and IL-23 (MesoScale Discovery) per the manufacturer's instructions. Supernatants were serially diluted based

on anticipated response. ELISAs were read on a SpectraMax® M5 Multi-Mode Microplate Reader at 450 nm. Cytokine concentration was determined by fitting standard curve OD values to a 4-parameter logistical model using curve fitting (XLFit, IDBS, Alameda, CA).

Supernatants from 72hr lymphocyte restimulation were analyzed using multiplex panel for murine analytes IFN- γ , IL-5, and IL-17 (MesoScale Discovery) per the manufacturer's instructions. Supernatants were run neat. Plates were read on a MESO QuickPlex SQ 120 instrument, and data were analyzed using Discovery Workbench (MesoScale Discovery).

In Vivo Experiments

Animal studies were carried out in an OLAW and AAALAC accredited vivarium in accordance with University of Montana's IACUC guidelines for the care and use of laboratory animals. Groups of 8 C57BL/6 mice were vaccinated intramuscularly with 1 μ g M72 antigen and indicated concentrations of adjuvants candidates in 50 μ l total volume per injection. After 28 days, blood and serum samples were collected, and a secondary vaccination was administered. At day 56 (28 days post-secondary vaccination), blood and serum samples were collected, and a tertiary vaccination administered. At day 70 (14 days post tertiary vaccination) mice were euthanized and blood was collected for the measurement of M72-specific humoral immunity. Spleens and lymph nodes were collected and homogenized for restimulation with antigen. Vaccination schedule and endpoints are detailed in Figure 9.

ELISA for anti-M72 antibody quantification.

Sera were collected and diluted according to the expected antibody response (between 1:10 and 1:5000). Plates were coated with 100 μ l of the full-length M72 protein

at 1 $\mu\text{g}/\text{mL}$. Following washing and blocking, plates were incubated with diluted serum for 1 hour followed by anti-mouse IgG, IgG1 or IgG2c-HRP secondary antibody (Bethyl Laboratories) and TMB substrate (KPL). Plates were read at 450 nm. Antibody titers were determined by fitting M72 specific positive control serum to a 4-parameter logistical model using curve fit software (XLFit, IDBS, Alameda, CA).

Lymphocyte restimulation and cell-mediated immunity analysis.

Spleens and lymph nodes were harvested from vaccinated mice 14 days after tertiary injections and lymphocytes were mechanically processed into a single cell suspension. Red blood cells were lysed by incubation with red blood cell lysis buffer (Sigma) for 5 min followed by washing in $1\times$ PBS. Cells were plated in a 96 well plate at 5×10^6 cells/well in 200 μL complete RPMI1640 media and incubated with 1 $\mu\text{g}/\text{mL}$ M72 antigen for either 6 hr or 72 hr at 37°C . Cells incubated for 72 hr were centrifuged and supernatants were collected for cytokine production. Cells incubated for 6 hr were treated with GolgiPlug (Brefeldin A, BD Biosciences) and incubated at 37°C for an additional 12 hr. Cells were then stained with the cell surface antibodies against CD3 BV605 (BD Horizons, 17A2), CD4 APC-R700 (Biolegend, GK1.5) and CD8a APC-Cy7 (Biolegend, 53–6.7) and viability stain (Ghost 510, Tonbo Biosciences). Cells were treated with cytofix/cytoperm (BD) and stained with anti-IFN- γ PE-CF594 (BD Biosciences, XMG1.2), anti-IL2 FITC (Biolegend, JES6–5H4), anti-IL-5 PE (BD Pharm, TRFK5), anti-IL-17A PerCP-Cy5.5 (Invitrogen, eBio17B7), and anti-TNF α PE-Cy7 (Biolegend, MP6-XT22). Data was collected using an LSRII flow cytometer (BD) and analyzed using FlowJo 10.0 software (TreeStar).

Statistical Analysis

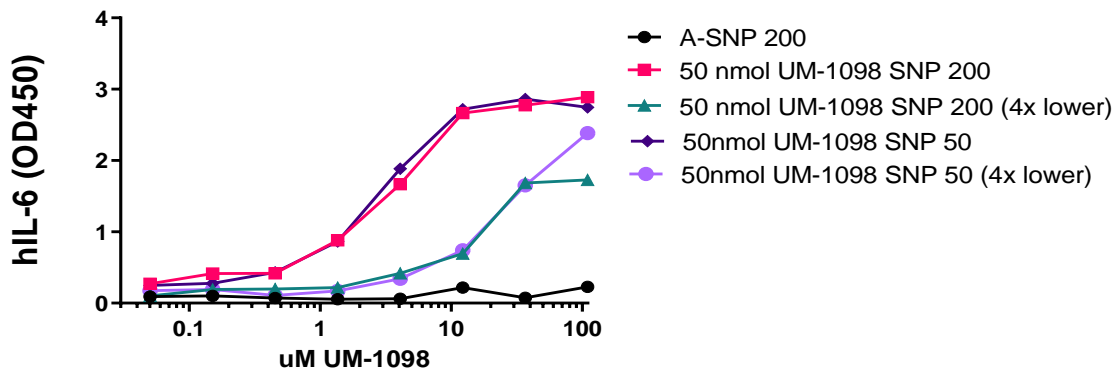
All statistical analyses were completed using GraphPad Prism 9.4.1. Nonlinear least squares regression of human PBMC dose response curves with a four-parameter variable slope was used to determine EC50 values and maximal cytokine output. Confidence intervals were calculated asymmetrically, and unstable parameters were identified and excluded. Best-fit values were compared using sum-of-squares F test. Antibody titers from mouse sera, flow cytometry population statistics, and T cell restimulation cytokines all were log transformed then subject to One-Way ANOVA with Tukey's post-hoc test.

CHAPTER 3: RESULTS

In Vitro Stimulation of Human PBMCs

We first set out to assess the impact of API coating density and silica nanoparticle size on UM-1098 potency. Coating density was tested in human PBMCs with normal (200nm particles at 10mg/mL A-SNP to 1mM API, 50nm particles at 2.5mg/mL A-SNP to 1mM API) and 4x lower coating densities (200nm particles at 40mg/mL A-SNP to 1mM API, 50nm particles at 10mg/mL A-SNP to 1mM API) comparing 50nm and 200nm A-SNPs in N=1 donors. Dose responses were observed to be dependent on coating density and independent of size. Coating densities of 200nm particles at 10mg/mL A-SNP to 1mM API or their 50nm particle counterparts at 2.5mg/mL A-SNP to 1mM API showed a superior UM-1098 dose response (Figure 5). Both assay performance and figure creation are credited to Cassandra Buhl (Figure 5).

Figure 5: Coating density dependent responses of UM-1098 on A-SNPs. Legend indicates starting concentrations of UM-1098 for each dose response curve. Figure created by Cassandra Buhl.



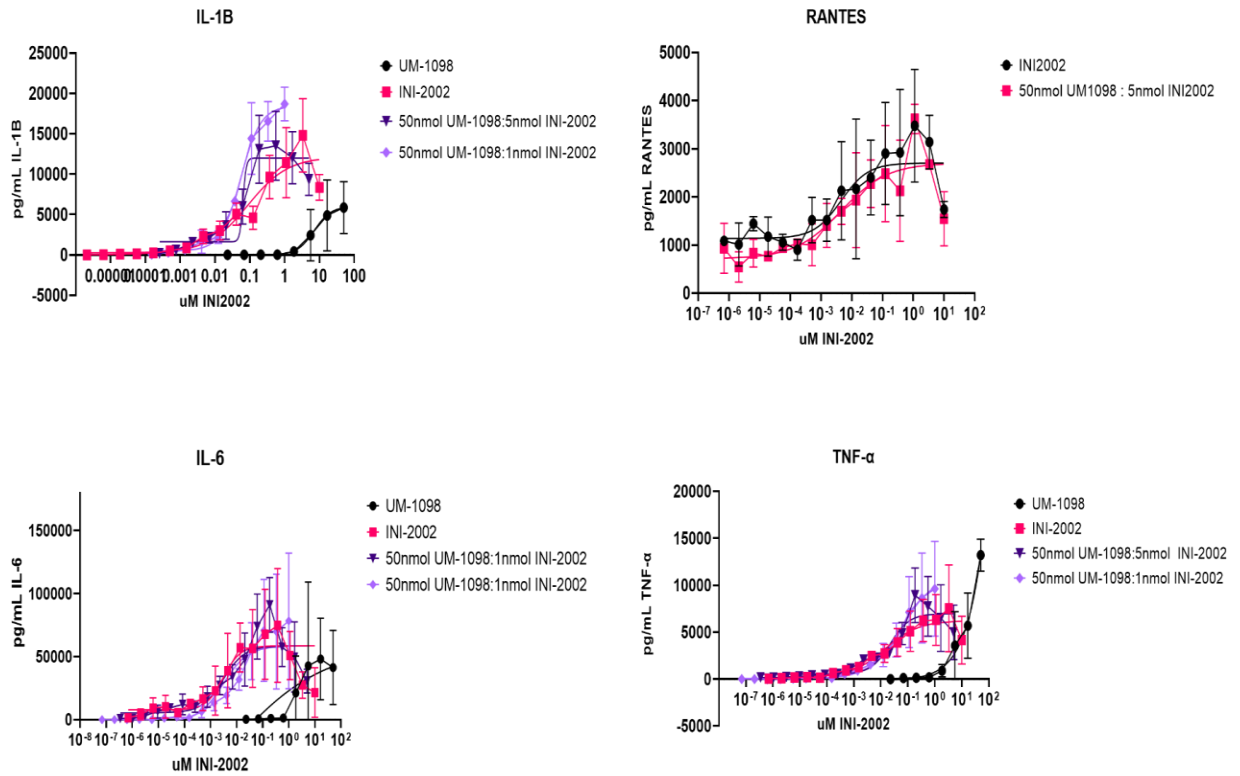
To determine efficacy of UM-1098 and INI-2002 combinations *in vitro*, dose response curves of UM-1098 and INI-2002 alone or combined in 50:1, 10:1, or 5:1 molar

ratio favoring UM-1098 were characterized for production of IL-1 β , TNF- α , IL-6, and RANTES in human PBMCs with N=3 donors (* indicates where N=2). Figure 6 provides a representative dose response for each cytokine profiled. Effective concentrations (EC50s) and maximum effect (Emax) were determined for each formulation and compared for significance using confidence intervals. UM-1098 was significantly less potent with a higher EC50 than all other formulations for every cytokine analyzed (p<0.05). Significant changes were not observed between EC50s for indicated cytokines in combination groups over INI-2002 alone. No EC50 was able to be generated from the UM-1098 dose response to TNF- α . Table 4 summarizes EC50 data.

	IL-1β		TNF-α		IL-6		RANTES	
	EC50 (uM)	CI95% (uM)	EC50 (uM)	CI95% (uM)	EC50 (uM)	CI95% (uM)	EC50 (uM)	CI95% (uM)
UM-1098	6.995	6.392 to 7.715	N/A	N/A	1.955	N/A	N/A	N/A
INI-2002	0.08970	0.01880 to 1.609	0.01405	0.002936 to 0.06835	0.001930	0.0001861 to 0.007607	0.004829*	0.0003185* to 0.04897*
50nmol UM-1098 : 10nmol INI-2002	0.08233	0.04249 to 0.1425	0.03795	0.006439 to N/A	0.002118	0.0002550 to 0.007658	N/A	N/A
50nmol UM-1098 : 5nmol INI-2002	0.04739	0.01964 to 0.09056	0.02217	0.006133 to 0.05780	0.003790	0.0008023 to 0.01268	0.004472*	0.0009055* to 0.02074*
50nmol UM-1098 : 1nmol INI-2002	0.05447	0.04185 to 0.07449	0.05922	0.01917 to 2977	0.01674	0.005130 to 2.871	N/A	N/A

Table 4: Effective Concentrations in Human PBMCs. N=3, * indicates where N=2. N/A=not assessed

Figure 6: Innate cytokine production in human PBMCs. N=3. Error bars represent SD.



Max cytokine production (E_{max}) of IL-1 β , TNF- α , IL-6, and RANTES results are tabulated in Table 5. IL-1 β E_{max} was significantly increased in the 50:1 molar ratio group in comparison to all other groups, with E_{max} of 18457pg/mL IL-1 β (CI: 16885-20711). TNF- α E_{max} was unable to be calculated for UM-1098.

	IL-1β		TNF-α		IL-6		RANTES	
	Emax (pg/mL)	CI95% (pg/mL)	Emax (pg/mL)	CI95% (pg/mL)	Emax (pg/mL)	CI95% (pg/mL)	Emax (pg/mL)	CI95% (pg/mL)
UM-1098	6001	5759 to 6275	N/A	N/A	45207	23332 to ???	N/A	N/A
INI-2002	12153	9511 to 21380	6222	5128 to 8349	50866	41025 to 61101	2821*	2360* to 3682*
50nmol UM-1098 : 10nmol INI-2002	10045	8815 to 11322	6361	5228 to 7526	59468	47040 to 72751	N/A	N/A
50nmol UM-1098 : 5nmol INI-2002	12085	10341 to 13962	6966	5932 to 8132	59570	50458 to 69177	2519*	2121* to 3354*
50nmol UM-1098: 1nmol INI-2002	18457	16885 to 20711	10959	8168 to 115266	80548	62770 to 212424	N/A	N/A

Table 5: Max cytokine output in human PBMCs. N=3, * indicates where N=2. N/A=not assessed

Inhibitive capacity was visualized through the application of a constant concentration of one active pharmaceutical ingredient (API) while the other was diluted in a dose response in human PBMCs. Addition of 1 μ M UM-1098 to varying concentrations of INI2002 did not result in reduced responses compared to 1 μ M UM-1098 alone among IFN α 2a, IL-6, TNF α , IL-1 β , IL-23, or IL-6 (Figure 7). Addition of 0.01 μ M INI-2002 to varying concentrations of UM-1098 was similarly performed and combination responses did not result in reduced responses compared to 0.01 μ M INI-2002 (Figure 8). The same experiment was completed with addition of 0.05 μ M INI-2002 to a UM-1098 dose response curve, and combination resulted in diminished IL-23 responses when compared to 0.05 μ M INI-2002 alone (Figure 9).

Figure 7: Constant addition of 1 μ M UM-1098 to INI-2002 dose response in human PBMCs. N=2.

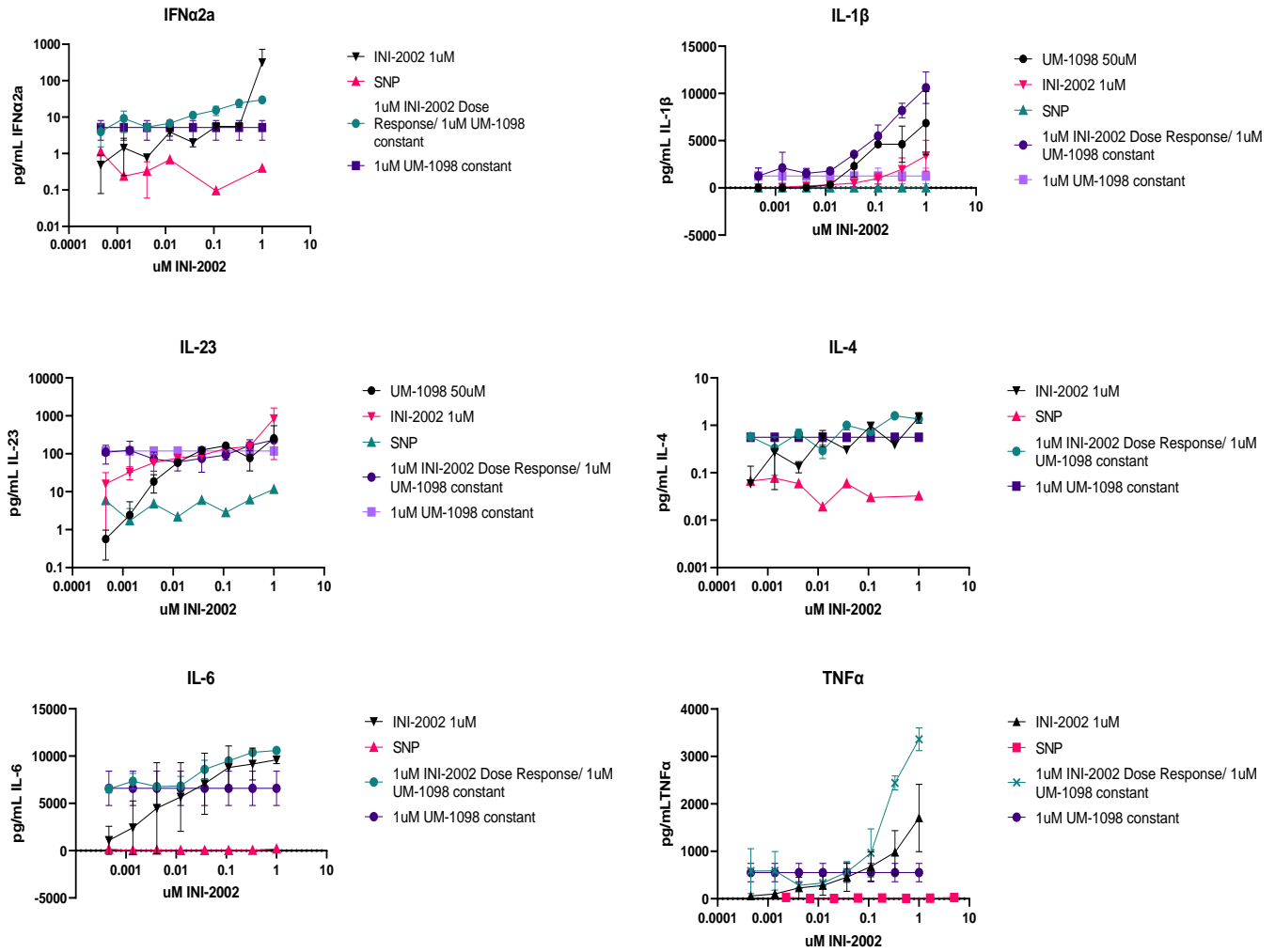


Figure 8: Constant addition of 0.01 μ M INI-2002 to UM-1098 dose response in human PBMCs. N=2.

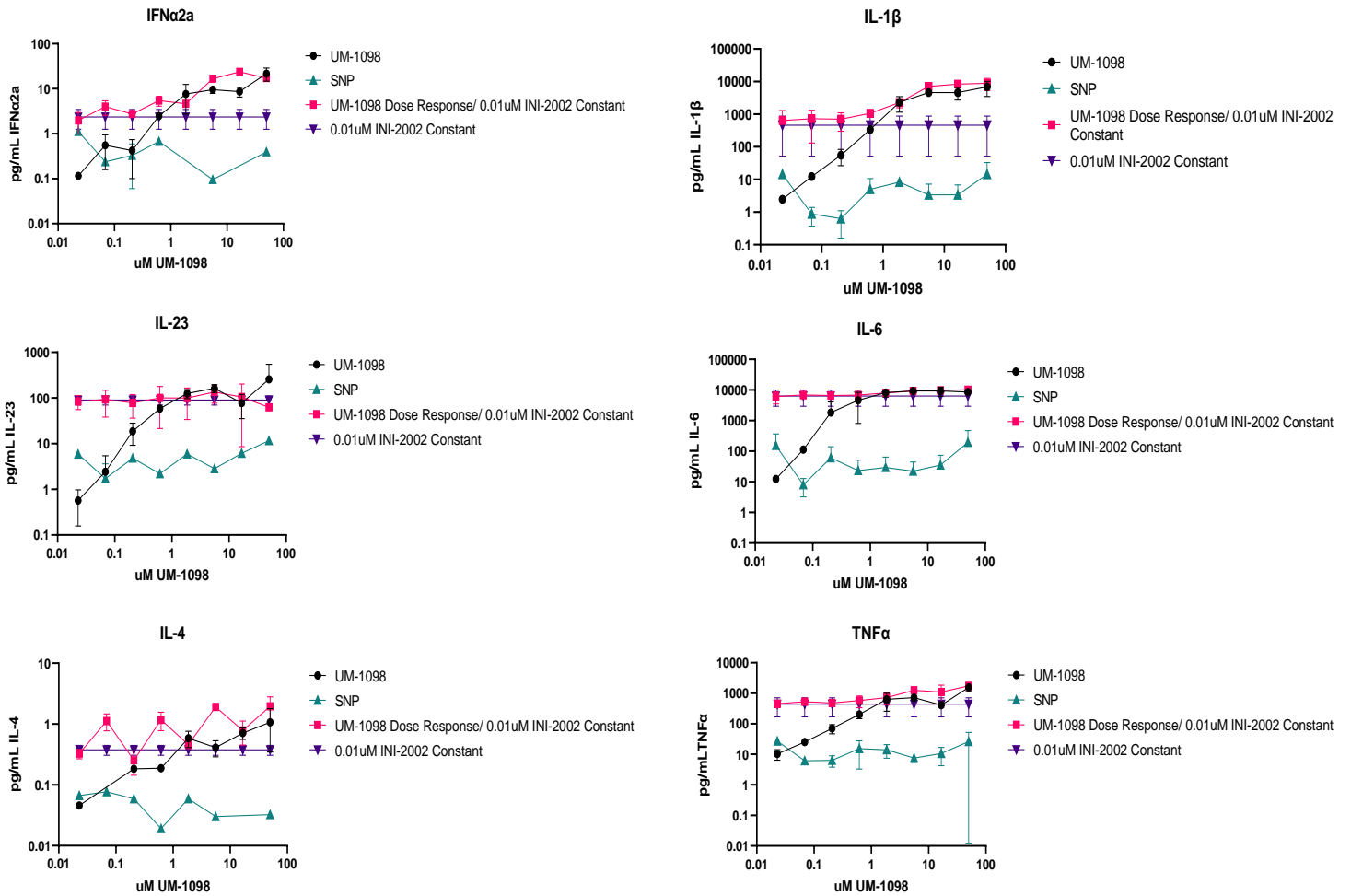
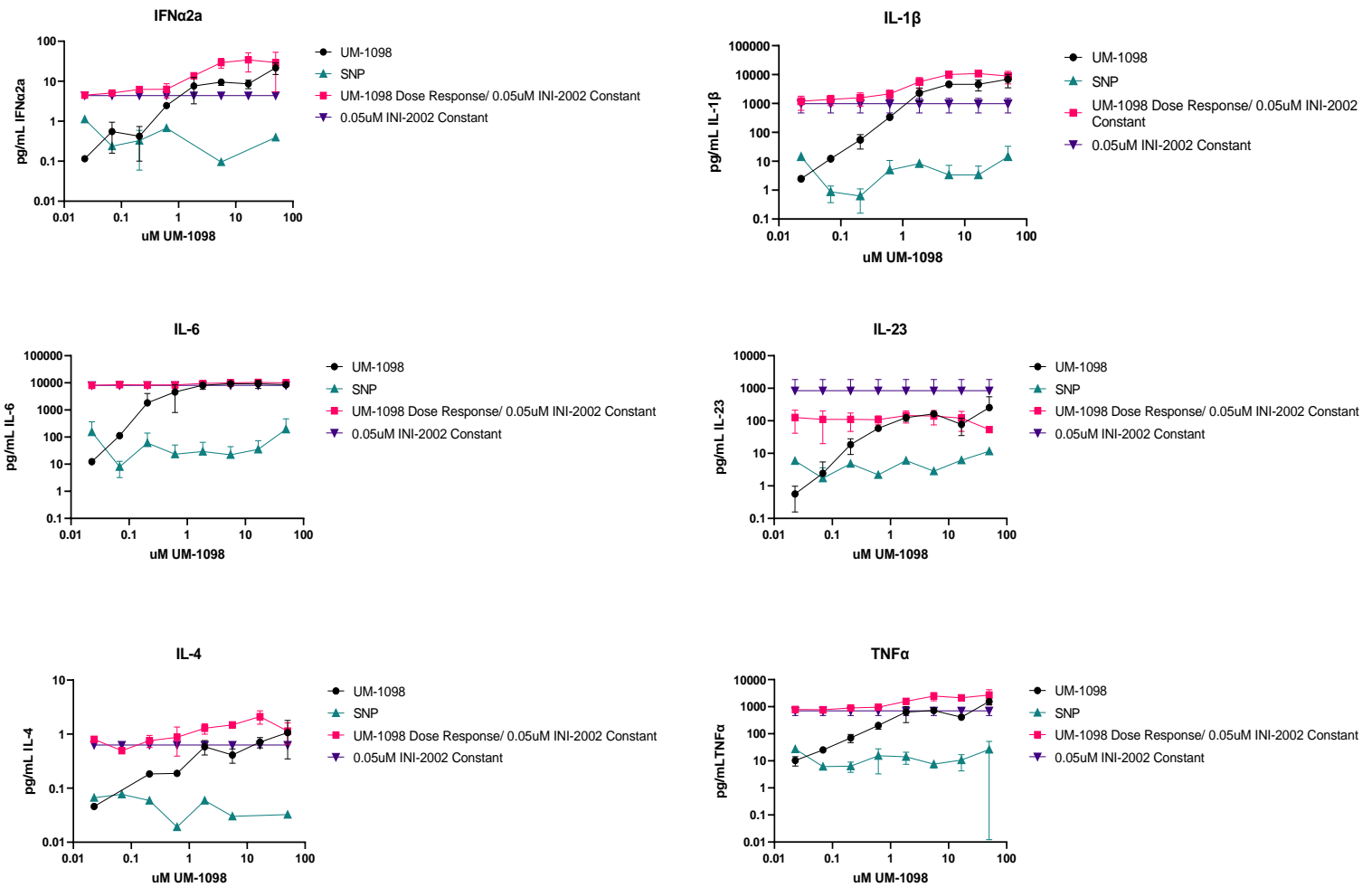


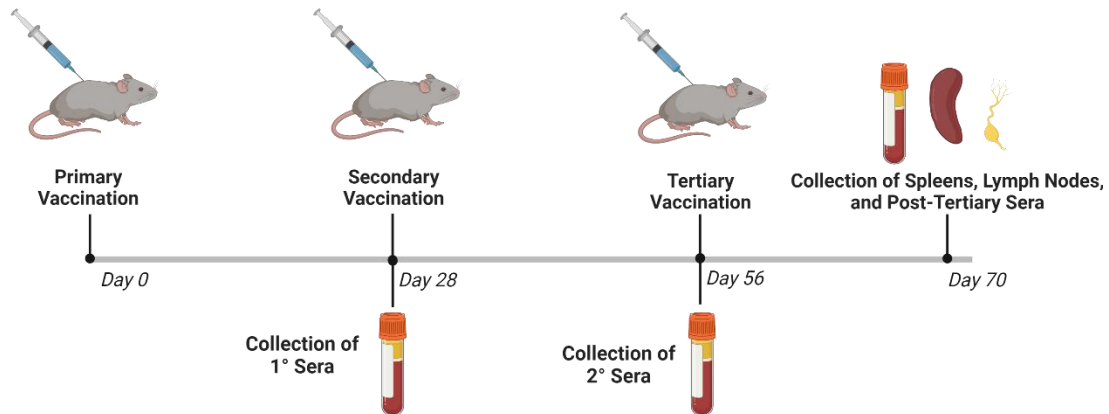
Figure 9: Constant addition of 0.05 μ M INI-2002 to UM-1098 dose response in human PBMCs. N=2.



In Vivo Vaccination of C57BL/6 Mice Against M72: Humoral Immunity

C57BL/6 mice were vaccinated against M72 antigen every 28 days and harvested 14 days post-tertiary vaccination. The vaccination schedule is demonstrated in Figure 9, and the vaccination conditions are tabulated in Table 6.

Figure 10: *In vivo* study schedule and endpoints



Antigen specific antibody titers were assessed by M72 ELISA and detected using IgG specific or IgG subclass specific antibodies. All mice receiving adjuvant produced significantly greater M72 specific antibody titers than antigen only. There were no observed differences in antibody responses between UM-1098 adsorbed to 50nm A-SNPs and UM-1098 adsorbed to 200nm A-SNPs, indicating no size-dependent response. Post-secondary IgG1 was increased among combination groups over INI-2002 alone (Figure 11C). The 10nmol UM-1098 : 1nmol INI-2002 combination group had increased IgG1 production over 10nmol UM-1098 at the post-secondary time point, although the 50nmol UM-1098 : 1nmol INI-2002 group did not have significantly increased titers over mice receiving 50nmol UM-1098 (Figure 11C). Notably, UM-1098 had significantly higher post-secondary IgG1 titers than INI-2002 (Figure 11C). All differences in IgG1 titers among adjuvanted groups were washed out at the post-tertiary time point (Figure 12B). No difference in antigen specific IgG2c titers was observed between adjuvanted groups at either time point (Figure 11B, Figure 12C). When observing antigen specific IgG titers without regard to serotype, both combination groups had increased IgG over INI-2002 treated mice but not over UM-1098 treated mice at the post-secondary time point (Figure

11A). Post-tertiary antigen specific IgG in mice treated with the 50nmol UM1098 : 1nmol INI-2002 combination was significantly higher than mice treated with UM-1098 alone but not mice treated with INI-2002 alone (Figure 12A). Mice adjuvanted with 10nmol UM-1098 and 1nmol INI-2002 had decreased IgG titers post-tertiary than when compared to IgG titers from the same mice at the post-secondary time point. This assay was repeated with similar results.

Description	# Mice	SNP Dose (ug)	UM-1098 Dose (nmol)	INI-2002 Dose (nmol)	M72 Dose (ug)
Naïve	6	-	-	-	-
A-SNP-50 Only	8	1000	-	-	-
Antigen Only	8	-	-	-	1
50nmol UM-1098-A-SNP-200	8	500	50	-	1
50nmol UM-1098-A-SNP-50	8	500	50	-	1
10nmol UM-1098-A-SNP-50	8	100	10	-	1
1nmol INI-2002-A-SNP-50	8	500	-	1	1
50nmol UM-1098-A-SNP-50 : 1nmol INI-2002-A-SNP-50	8	1000	50	1	1
10nmol UM-1098-A-SNP-50 : 1nmol INI-2002-A-SNP-50	8	600	50	1	1

Table 6: *In vivo* study conditions

Figure 11: Post-secondary antibody titers. Asterisks indicate significance where * $p < 0.05$, ** $p < 0.01$, *** $p < 0.001$, **** $p < 0.0001$, # indicates antigen only group is significantly different than all groups indicated under bracket where $p < 0.05$. N=8

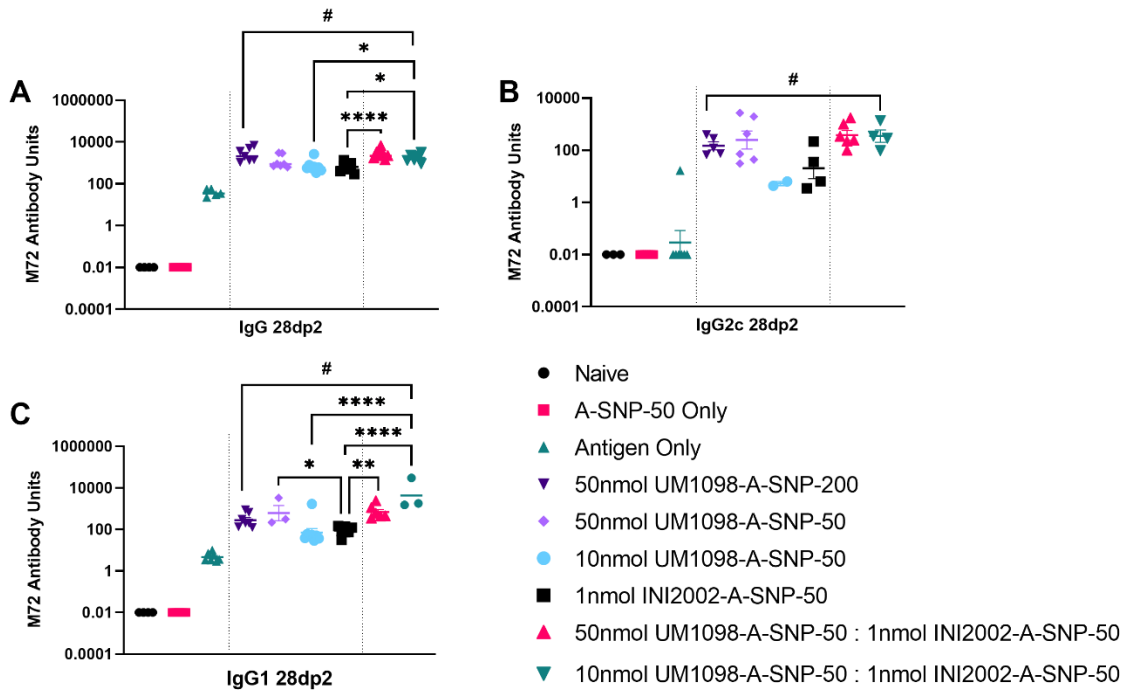
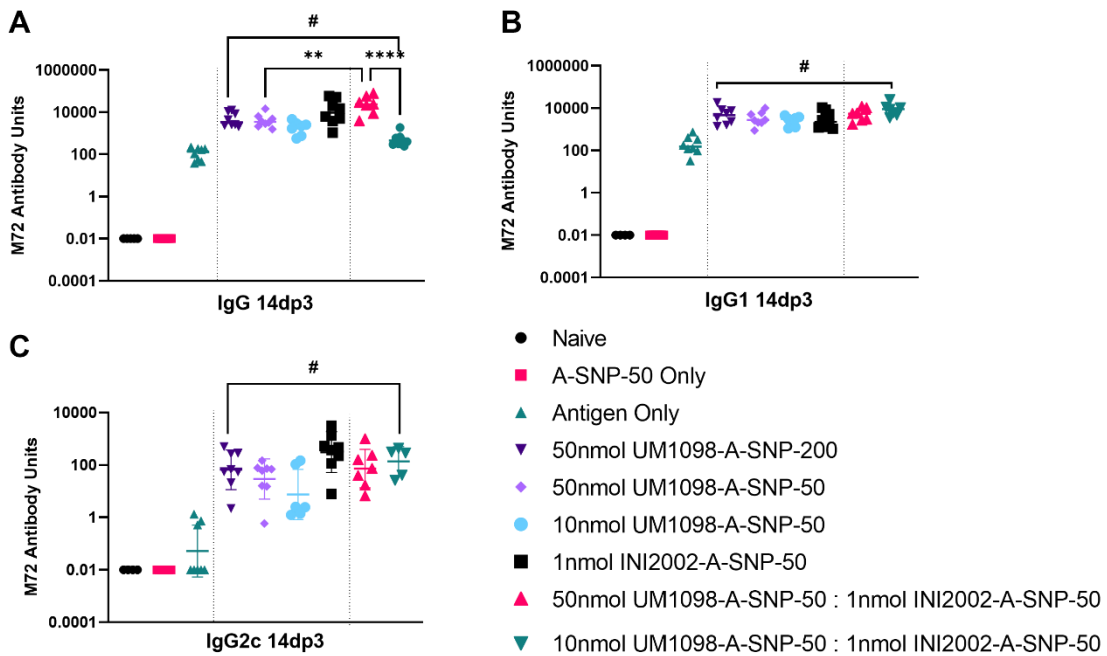


Figure 12: Post-tertiary antibody titers. Asterisks indicate significance where * $p < 0.05$, ** $p < 0.01$, *** $p < 0.001$, **** $p < 0.0001$, # indicates antigen only group is significantly different than all groups indicated under bracket where $p < 0.05$. N=8



In Vivo Vaccination of C57BL/6 Mice Against M72: Cell-Mediated Immunity

Mouse lymph nodes and spleens were homogenized into single cell suspensions then restimulated with antigen for determination of M72-specific T cell responses. Restimulated cells were stained for CD3, CD4, CD8, IFN- γ , TNF- α , IL-2, IL-5, and IL-17 to be detected via flow cytometry. A representative gating strategy is depicted in Figure 13. Neither the lymphocytes from the lymph nodes (LN) or spleens displayed noticeable changes in IL-5⁺ CD4⁺ T cells upon restimulation, even above that of antigen alone (Figure 14 Panel C). Mice stimulated with 10nmol UM-1098 : 1nmol INI-2002 showed significantly higher rates of TNF- α ⁺ and IFN- γ ⁺ CD4⁺ T cells in the lymph node when compared to mice receiving UM-1098 only or the 50:1 molar ratio combination (Figure 14 Panel D and E). No significant differences were seen in IL-17⁺ T cells among adjuvanted groups in the LN although all were significantly different than antigen only (Figure 14 Panel A). A trend towards more IL-17⁺ CD4⁺ splenocytes among combination adjuvants was seen in comparison to mice adjuvanted with UM-1098-A-SNP-200 or given antigen only. In comparing UM-1098 on 200nm SNPs vs 50nm SNPs, the only observable difference was increased TNF- α producing cells in splenocytes treated with UM-1098 on the 50nm size (Figure 14 Panel D). INI-2002 produced significantly more TNF- α ⁺ and IL-2⁺ antigen specific T cells in the spleen than UM-1098 counterparts (Figure 14 Panel B and D).

Lymphocytes isolated from the spleens and lymph nodes were incubated with antigen for 72hr and analyzed for adaptive T cell cytokines in cell supernatants. The 10:1 molar ratio combination was the most potent inducer of IFN- γ among all splenocyte

supernatants and showed statistical significance above all other groups (Figure 15). Production of IFN- γ in lymph node restimulation supernatants was significantly lower in the 10nmol UM-1098 group than all other adjuvanted groups (Figure 15). IL-5 production upon restimulation was not significantly different among any groups in spleen or lymph node cultures above naïve or antigen stimulated groups (Figure 15). Secreted IL-17 in lymph node restimulation supernatants was significantly higher in the 10:1 molar ratio combination than either the 10nmol UM-1098 or 1nmol INI-2002 groups (Figure 15). Splenocytes similarly had increased IL-17 recall in the 50:1 molar ratio combination in comparison to UM-1098 groups (Figure 15).

Figure 13: Representative T Cell Gating Strategy. Lymphocytes were gated for live dead exclusion dye, followed by a singlet gate, a CD3 gate, and then for CD4 or CD8 phenotypes. Cells were then gated for intracellular cytokine production.

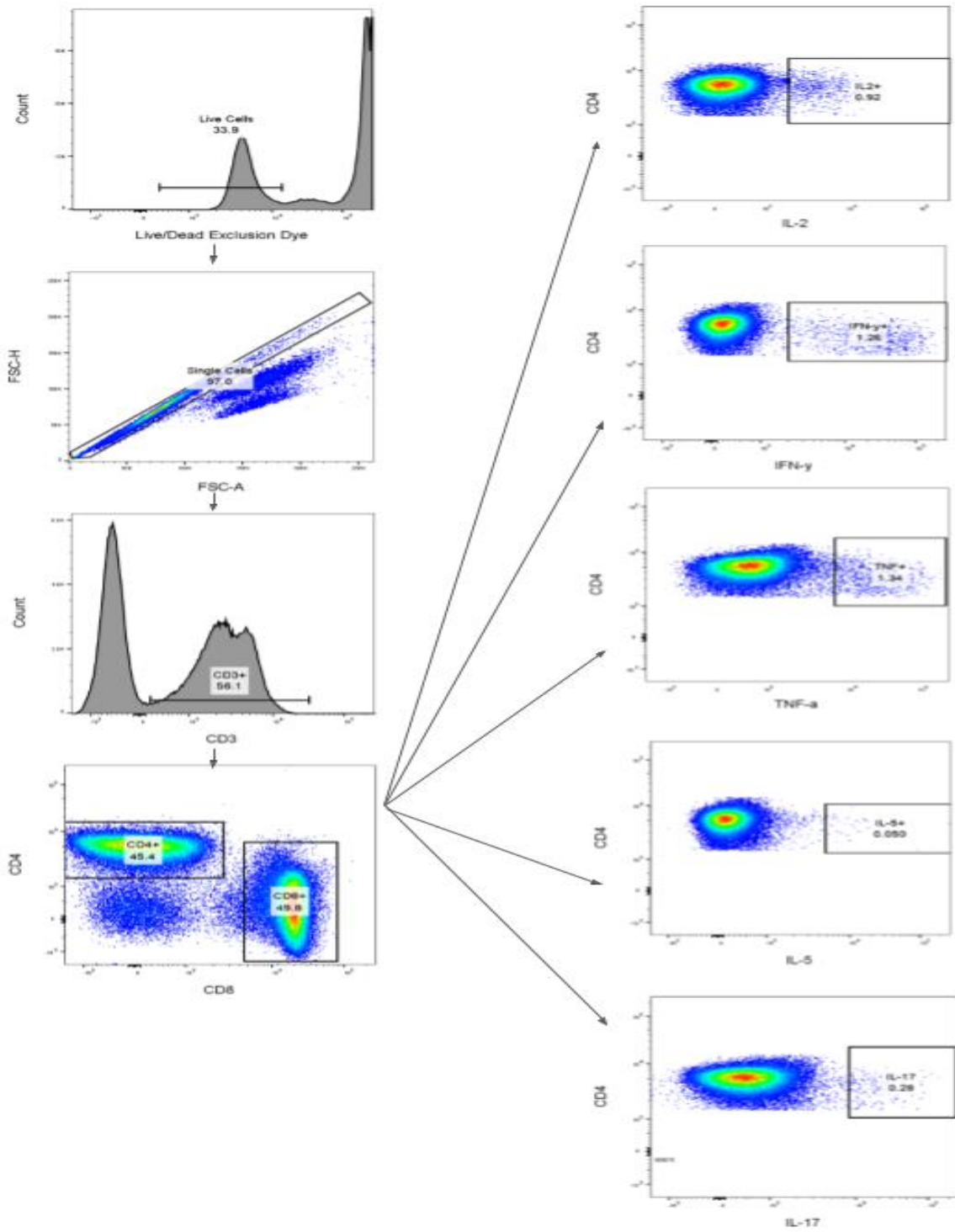


Figure 14: Combination vaccination increases percentage of antigen specific CD4+ T Cells Producing Th1 Biasing Cytokines. Intracellular cytokines IL-17a (A), IL-2 (B), IL-5 (C), TNF- α (D), and IFN- γ (E) were measured via flow cytometry. Data represents percent of total CD3+CD4+ population which produce indicated cytokine. Lines indicate means. Data was log transformed and analyzed via one-way ANOVA with Tukey's post-hoc test (GraphPad Prism 9); asterisks indicate significance where * p <0.05, ** p <0.01, *** p <0.001, # indicates antigen only group is significantly different than all groups indicated under bracket where p <0.05. Asterisks indicate significance where * p <0.05, ** p <0.01, *** p <0.001, **** p <0.0001, # indicates antigen only group is significantly different than all groups indicated under bracket where p <0.05. N=8

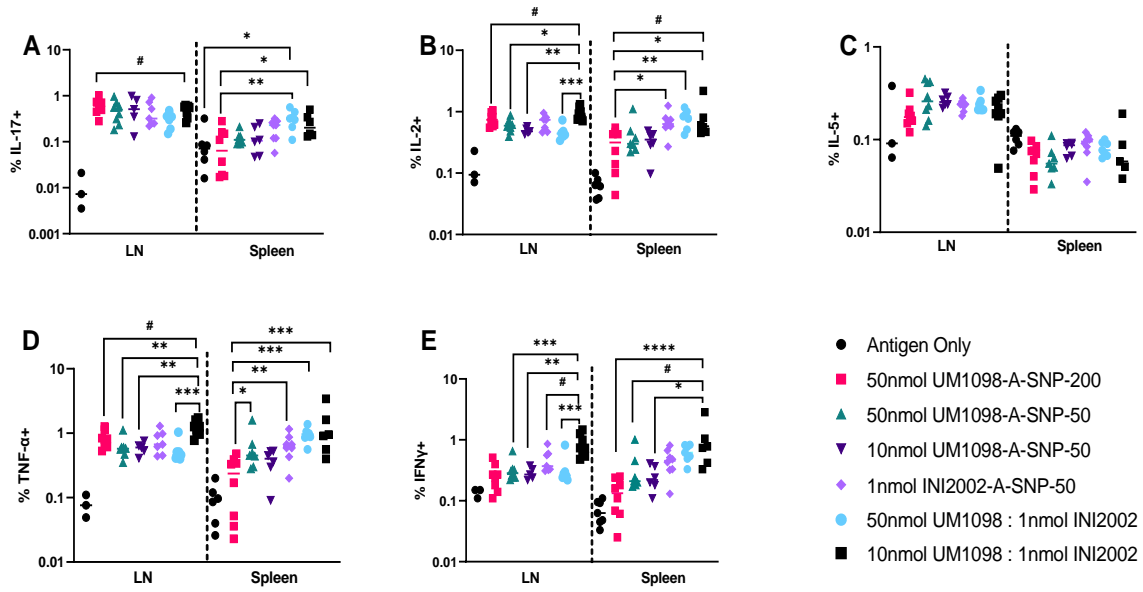
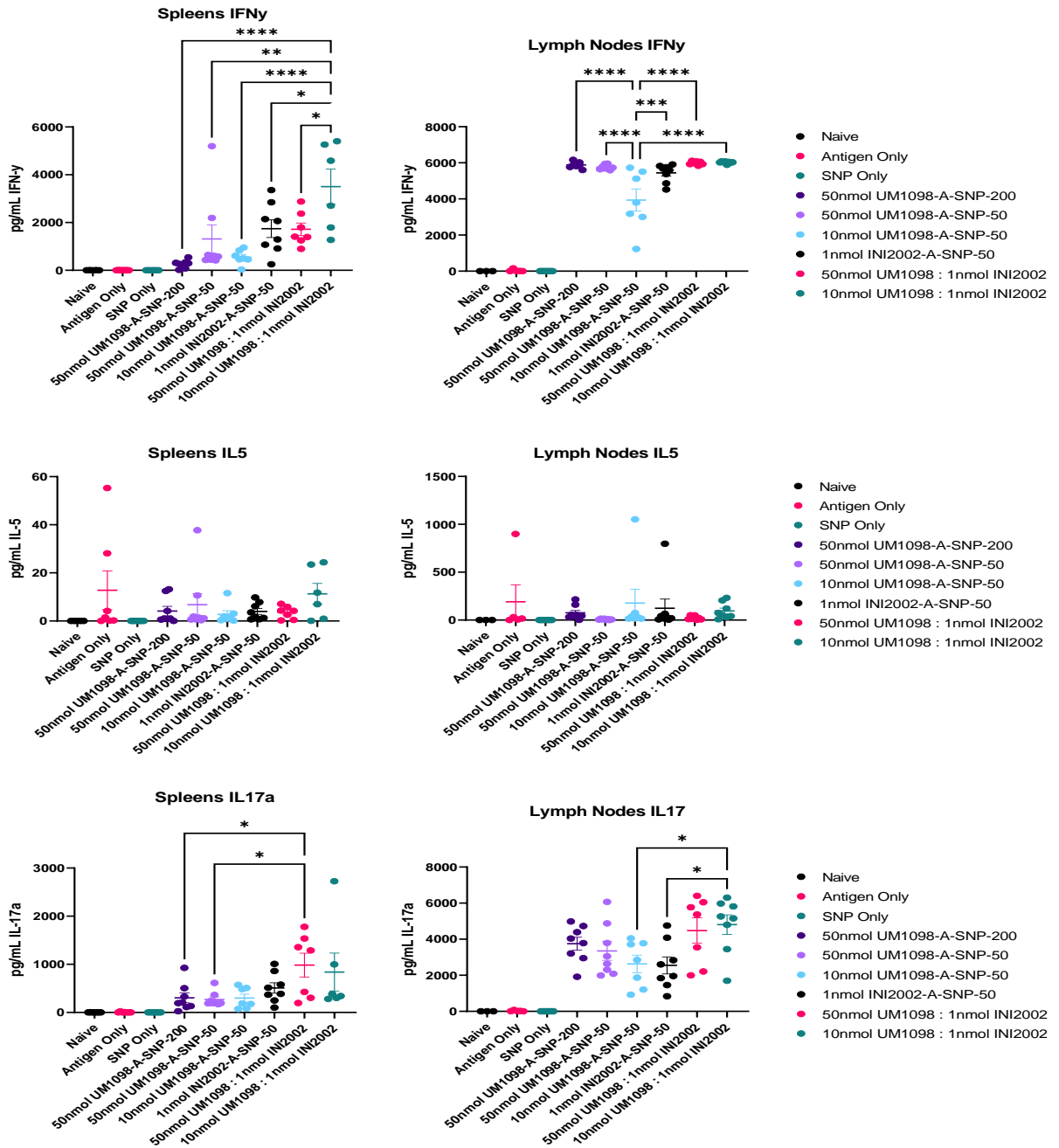


Figure 15: Combination Vaccination Increases IL-17 and IFN- γ Recall Upon Splenocyte Restimulation. N=8. Asterisks indicate significance where * $p < 0.05$, ** $p < 0.01$, *** $p < 0.001$, **** $p < 0.0001$.



CHAPTER 4: DISCUSSION

The characterization of UM-1098 coated to A-SNPs *in vitro* successfully detected several important properties to take into consideration when designing future formulations of UM-1098 as well as other Mincle ligands. Coating density of UM-1098 on A-SNPs was shown to be directly related to potency, which was determined to be independent of A-SNP diameter (Figure 5). This finding supported the hypothesis that stabilization of Mincle ligands on a silica nanoparticle enables UM-1098 to form multiple PRR-ligand interactions for more potent signaling similar to the mechanism previously described with Dectin-1 (50). Comparisons of mice vaccinated against M72 antigen adjuvanted with UM-1098 on 50nm or 200nm A-SNPs found no significant difference in humoral adaptive immune responses when dose of API and SNP were kept constant, further demonstrating that signaling was independent of carrier particle size (Figures 11 and 12). In comparing the cell-mediated immune responses to UM-1098 on 200nm SNPs vs 50nm SNPs, the only observable difference was increased TNF- α + CD4+ splenocytes treated with UM-1098 on the 50nm size (Figure 14 Panel D). Though this difference may appear size dependent, it's important to note that the dose of both UM-1098 as well as A-SNP was held constant. The same dose by weight of A-SNPs at a 50nm diameter has significantly more surface area than the same dose by weight of 200nm diameter A-SNPs, meaning that the 50nm group was at a lower coating density and observes the same trend as seen *in vitro*. Formation of so-called "signalosomes" with Mincle ligands has not been published; further investigation and understanding of this phenomenon would contribute significantly to adjuvant design.

Several clinically evaluated or licensed vaccines have been adjuvanted with multiple PRR ligands for broader cell-mediated immune responses. Several of these

combinations have utilized TLR4 agonist MPL including the M72/AS01E vaccine which induced strong Th1 biased immunity. Although Mincle ligands including TDB have been investigated clinically for their ability to induce Th17 responses, these agonists have yet to be clinically tested in dual agonist vaccine formulations. Combination of Mincle and TLR4 agonists TDB and MPL respectively administered in DDA liposomes has been demonstrated to increase production of IFN- γ , IL-2, TNF- α , and IL-17A *in vivo*. We reformed this design with a rational approach to increased stability and safety while minimizing toxicity. Adjuvants with shorter fatty acid chain lengths including INI-2002 and novel Mincle agonist UM-1098 were chosen, and SNPs were chosen as a carrier molecule for controlled coating density and improved shelf life. When these combinations were assessed *in vitro*, though combination of UM-1098 and INI-2002 did not significantly change the EC50s of any cytokines assessed, synergy was observed in increased total IL-1 β output by 50:1 molar ratio combination (Figure 6). Increasing power by including more donors may have increased statistical significance in Emax or EC50 among other cytokines.

Working doses of the selected agonists were assessed for inhibitive capacity *in vitro* to observe if Mincle-regulated suppression of TLR4 coreceptor CD14 would impact efficacy. Inhibition of the UM-1098 dose response as measured by IFN α 2a, IL-6, TNF α , IL-1 β , IL-23, and IL-6 was not observed following addition of a constant 0.01 μ M INI-2002 to each point of the UM-1098 dose curve (Figure 8). Interestingly, addition of 0.05 μ M INI2002 to the UM-1098 dose response curve improved IL-23 over UM-1098 alone, but cytokine production was lower than that of 0.05 μ M INI-2002 alone, indicating these responses were less than additive (Figure 9). Addition of 1 μ M UM-1098 to INI-2002 dose

response curves did not indicate anything less than additive responses (Figure 7). Overall, these data suggest at least additive responses for all cytokines assessed other than IL-23 production, and it's predicted that inhibition of other cytokines occurs at molar ratios outside of the working range of the selected adjuvants.

Adaptive immune responses were assessed *in vivo* for both the characterization of UM-1098 adsorbed to 50nm or 200nm A-SNPs as well as the characterization of combinatorial administration of UM-1098 and INI-2002. Two combination groups were investigated, one of which was based on previously determined optimal doses of each compound (50nmol UM-1098 and 1nmol INI-2002) as well as a dose spared group with the optimal dose of INI-2002 and a 5-fold reduction in UM-1098 dose (10nmol UM-1098 and 1nmol INI-2002). No difference was observed in humoral responses assessed by antibody titers between UM-1098 administered at a fixed dose on 200nm or 50nm A-SNPs, suggesting that responses were independent of carrier particle diameter (Figures 11 and 12). Post-secondary antibody responses showed that combination administration was able to increase antigen specific IgG1 and IgG titers compared to those generated in singly adjuvanted mice (Figure 11). These results were washed out in post-tertiary sera (Figure 12), however, it's important to note that clinical vaccines rarely employ tertiary injections, and the post-secondary sera are more representative of clinical efficacy. The increase in IgG1 among dual-adjuvanted groups was unexpected; bias towards IgG1 is generally associated with Th2 type responses. This finding is especially odd given that it conflicts with T cell cytokine data which suggests a Th1 polarized response. Finally, the decrease in post-tertiary IgG titers seen in the 10:1 molar ratio is likely a human error considering that the same mice had notably higher titers only a month before. M72 specific antibody

quantification was repeated on these samples with a new standard and similar results were yielded. The ongoing *Mtb* challenge study will serve as a repetition to validate these data. Further investigation into class switching as well as the analysis of antigen-specific IgA responses would benefit understanding of humoral responses in Mincle and TLR4 combination groups.

Th1 and Th17 biased cell-mediated immunity is the strongest correlate of protection against pulmonary tuberculosis. We hypothesized that combination of Th1/17 biasing agonist INI-2002 with Th17 biasing agonist UM-1098 would yield potent Th1 and Th17 memory, and that Mincle signaling would be independent of carrier particle size. Identification of cytokine producing antigen specific T cells via flow cytometry as well as analysis of T cell cytokines following restimulation both indicated no changes in Th2 biasing cytokine IL-5 among any adjuvanted groups (Figures 14 and 15). In assessment of Th1 associated cytokines we found that mice stimulated with the 10nmol UM-1098 : 1nmol INI-2002 combination had the most TNF- α ⁺ and IFN- γ ⁺ CD4⁺ T cells as observed by flow cytometry, with more potent responses than the 50nmol UM-1098 : 1nmol INI-2002 combination group (Figure 14 Panel D and E). Similarly, mice receiving the 10:1 molar ratio combination produced the strongest IFN- γ recall among all splenocyte supernatants and showed statistical significance above all other groups (Figure 15). Though no differences in IL-17⁺ CD4⁺ T cells was seen among adjuvanted groups in the lymph nodes, combination groups yielded increased numbers of IL-17⁺ CD4⁺ splenocytes in comparison to UM-1098-A-SNP-200 and antigen only groups (Figure 14 Panel A). More promisingly, secreted IL-17 in lymph node restimulation supernatants was significantly higher in the 10:1 molar ratio combination than either the 10nmol UM-1098 or 1nmol INI-2002 groups

(Figure 15). Splenocytes similarly had increased IL-17 recall in the 50:1 molar ratio combination in comparison to UM-1098 groups (Figure 15).

Taken together these data suggest the 10:1 molar ratio combination as the most potent adjuvant formulation for Th1/Th17 biased immunity. This group was originally designed with dose-sparing in mind, hypothesizing that through synergy this formulation could do just as well as the 50nmol UM-1098 : 1 nmol INI-2002 combination group (as determined by no statistically significant differences between the two groups). Instead, the dose-spared group produced more potent Th1 responses than the group receiving a 50:1 molar ratio. It's possible that Mincle dependent downregulation of TLR4 coreceptor CD14 partially reduced responses in the 50:1 molar ratio group. Analyzing expression profiles of CD14 after combinatorial vaccination *in vivo* could more conclusively determine if higher concentrations of Mincle are responsible for the partial ablation of synergy in adaptive immune responses seen in the group receiving 50nmol UM-1098 : 1nmol INI-2002.

CHAPTER 5: CONCLUSIONS

Summary of Findings

Mincle agonist UM-1098 signaling is dependent on coating density on the delivery vehicle. Combination of TLR4 adjuvant INI-2002 and Mincle adjuvant UM-1098 delivered admixed on A-SNPs results in increased IL-1 β secretion *in vitro* and produced potent Th1/Th17 immune responses *in vivo*. Mincle and TLR4 were determined to work additively at low doses for induction of innate cytokines IL-6, IL-1 β , TNF- α , and IFN α 2a, but not for IL-23. Synergistic adaptive immune responses allowed for a five-fold reduction in UM-1098 usage in vaccine formulations with as good or better responses than combinations given at full dosage. Mice vaccinated against M72 and adjuvanted with 10nmol UM-1098 and 1nmol INI-2002 showed increased TNF- α +, IL-17+, and IFN- γ + CD4+ T cells as observed by flow cytometry, as well as potent IFN- γ and IL-17 recall in restimulation supernatants.

Future Directions

An ongoing murine *Mtb* challenge aims to compare previously characterized 10nmol UM-1098 : 1nmol INI-2002 combinations versus BCG. Outputs to be assessed include IgG titers and subtypes, T cell restimulation responses, lung and spleen colony forming unit counts, and histology of lungs post-challenge. Future *in vivo* studies will include *Mincle* *-/-* and *TLR4* *-/-* mice from a C57BL/6 background to determine if synergy is specific to Mincle and TLR4.

Stimulation of human PBMCs with UM-1098 or INI-2002 adsorbed to fluorescently labeled silica nanoparticles followed by cell phenotyping and intracellular cytokine staining will aid in understanding which cells are responsible for the synergistic

innate immune response. Comparisons of INI-2002 and UM-1098 admixed versus co-adsorbed to the same particle may also show enhanced responses, as has been demonstrated for TLR4 and TLR7/8 agonists. Data for EC50 and Emax values will be expanded by testing additional donors.

BIBLIOGRAPHY

1. Global Tuberculosis Report 2021 [Internet]. [cited 2022 Aug 6]. Available from: <https://www.who.int/teams/global-tuberculosis-programme/tb-reports/global-tuberculosis-report-2021>
2. Medicine (US) I of. The Global Burden of Drug-Resistant TB [Internet]. Facing the Reality of Drug-Resistant Tuberculosis in India: Challenges and Potential Solutions: Summary of a Joint Workshop by the Institute of Medicine, the Indian National Science Academy, and the Indian Council of Medical Research. National Academies Press (US); 2012 [cited 2022 Aug 17]. Available from: <https://www.ncbi.nlm.nih.gov/books/NBK100388/>
3. Burki TK. The global cost of tuberculosis. *Lancet Respir Med*. 2018 Jan 1;6(1):13.
4. Hunter RL. The Pathogenesis of Tuberculosis: The Early Infiltrate of Post-primary (Adult Pulmonary) Tuberculosis: A Distinct Disease Entity. *Front Immunol*. 2018 Sep 19;9:2108.
5. Jilani TN, Avula A, Zafar Gondal A, Siddiqui AH. Active Tuberculosis. In: *StatPearls* [Internet]. Treasure Island (FL): StatPearls Publishing; 2022 [cited 2022 Aug 14]. Available from: <http://www.ncbi.nlm.nih.gov/books/NBK513246/>
6. Ehlers S, Schaible UE. The granuloma in tuberculosis: dynamics of a host-pathogen collusion. *Front Immunol*. 2012;3:411.
7. Mbuh TP, Ane-Anyangwe I, Adeline W, Thumamo Pokam BD, Meriki HD, Mbacham WF. Bacteriologically confirmed extra pulmonary tuberculosis and treatment outcome of patients consulted and treated under program conditions in the littoral region of Cameroon. *BMC Pulm Med*. 2019 Jan 17;19(1):17.
8. Pang Y, An J, Shu W, Huo F, Chu N, Gao M, et al. Epidemiology of Extrapulmonary Tuberculosis among Inpatients, China, 2008–2017. *Emerg Infect Dis*. 2019 Mar;25(3):457–64.
9. J L, L Z, C Q. The double-sided effects of Mycobacterium Bovis bacillus Calmette-Guérin vaccine. *NPJ Vaccines* [Internet]. 2021 Jan 25 [cited 2022 Aug 13];6(1). Available from: <https://pubmed.ncbi.nlm.nih.gov/33495451/>
10. Mangtani P, Abubakar I, Ariti C, Beynon R, Pimpin L, Fine PEM, et al. Protection by BCG Vaccine Against Tuberculosis: A Systematic Review of Randomized Controlled Trials. *Clin Infect Dis*. 2014 Feb 15;58(4):470–80.

11. Nieuwenhuizen NE, Kulkarni PS, Shaligram U, Cotton MF, Rentsch CA, Eisele B, et al. The Recombinant Bacille Calmette-Guérin Vaccine VPM1002: Ready for Clinical Efficacy Testing. *Front Immunol.* 2017;8:1147.
12. Marinova D, Gonzalo-Asensio J, Aguilo N, Martin C. MTBVAC from discovery to clinical trials in tuberculosis-endemic countries. *Expert Rev Vaccines.* 2017 Jun;16(6):565–76.
13. Burchill MA, Tamburini BA, Pennock ND, White JT, Kurche JS, Kedl RM. T cell Vaccinology: Exploring the known unknowns. *Vaccine.* 2013 Jan 2;31(2):297–305.
14. Vaccine Types | NIH: National Institute of Allergy and Infectious Diseases [Internet]. [cited 2022 Aug 14]. Available from: <https://www.niaid.nih.gov/research/vaccine-types>
15. Nemes E, Geldenhuys H, Rozot V, Rutkowski KT, Ratangee F, Bilek N, et al. Prevention of *M. tuberculosis* Infection with H4:IC31 Vaccine or BCG Revaccination. *N Engl J Med.* 2018 Jul 12;379(2):138–49.
16. Tait DR, Hatherill M, Van Der Meeren O, Ginsberg AM, Van Brakel E, Salaun B, et al. Final Analysis of a Trial of M72/AS01E Vaccine to Prevent Tuberculosis. *N Engl J Med.* 2019 Dec 19;381(25):2429–39.
17. McShane H. Insights and challenges in tuberculosis vaccine development. *Lancet Respir Med.* 2019 Sep 1;7(9):810–9.
18. Darrah PA, Zeppa JJ, Maiello P, Hackney JA, Wadsworth MH, Hughes TK, et al. Prevention of tuberculosis in macaques after intravenous BCG immunization. *Nature.* 2020 Jan;577(7788):95–102.
19. Rn C, Ta D, R E, Fm P, Am B, J V, et al. The TLR-4 agonist adjuvant, GLA-SE, improves magnitude and quality of immune responses elicited by the ID93 tuberculosis vaccine: first-in-human trial. *NPJ Vaccines* [Internet]. 2018 Sep 4 [cited 2022 Aug 14];3. Available from: <https://pubmed.ncbi.nlm.nih.gov/30210819/>
20. van Dissel JT, Joosten SA, Hoff ST, Soonawala D, Prins C, Hokey DA, et al. A novel liposomal adjuvant system, CAF01, promotes long-lived Mycobacterium tuberculosis-specific T-cell responses in human. *Vaccine.* 2014 Dec 12;32(52):7098–107.
21. Deng J, Bi L, Zhou L, Guo S juan, Fleming J, Jiang H wei, et al. Mycobacterium Tuberculosis Proteome Microarray for Global Studies of Protein Function and Immunogenicity. *Cell Rep.* 2014 Dec 24;9(6):2317–29.
22. Skeiky YAW, Lodes MJ, Guderian JA, Mohamath R, Bement T, Alderson MR, et al. Cloning, Expression, and Immunological Evaluation of Two Putative Secreted Serine Protease Antigens of Mycobacterium tuberculosis. *Infect Immun.* 1999 Aug;67(8):3998–4007.

23. Rodo MJ, Rozot V, Nemes E, Dintwe O, Hatherill M, Little F, et al. A comparison of antigen-specific T cell responses induced by six novel tuberculosis vaccine candidates. *PLoS Pathog.* 2019 Mar 4;15(3):e1007643.
24. Zhu B, Dockrell HM, Ottenhoff THM, Evans TG, Zhang Y. Tuberculosis vaccines: Opportunities and challenges. *Respirology.* 2018;23(4):359–68.
25. Golubovskaya V, Wu L. Different Subsets of T Cells, Memory, Effector Functions, and CAR-T Immunotherapy. *Cancers.* 2016 Mar 15;8(3):36.
26. Kuby, J. *Immunology.* New York: W.H. Freeman; 1997.
27. Ciesielska A, Matyjek M, Kwiatkowska K. TLR4 and CD14 trafficking and its influence on LPS-induced pro-inflammatory signaling. *Cell Mol Life Sci.* 2021 Feb 1;78(4):1233–61.
28. Didierlaurent AM, Morel S, Lockman L, Giannini SL, Bisteau M, Carlsen H, et al. AS04, an Aluminum Salt- and TLR4 Agonist-Based Adjuvant System, Induces a Transient Localized Innate Immune Response Leading to Enhanced Adaptive Immunity. *J Immunol.* 2009 Nov 15;183(10):6186–97.
29. Garçon N, Di Pasquale A. From discovery to licensure, the Adjuvant System story. *Hum Vaccines Immunother.* 2016 Sep 16;13(1):19–33.
30. Mata-Haro V, Cekic C, Martin M, Chilton PM, Casella CR, Mitchell TC. The vaccine adjuvant monophosphoryl lipid A as a TRIF-biased agonist of TLR4. *Science.* 2007 Jun 15;316(5831):1628–32.
31. Gao J, Guo Z. Progress in the Synthesis and Biological Evaluation of Lipid A and Its Derivatives. *Med Res Rev.* 2018 Mar;38(2):556–601.
32. Short KK, Lathrop SK, Davison CJ, Partlow HA, Kaiser JA, Tee RD, et al. Using Dual Toll-like Receptor Agonism to Drive Th1-Biased Response in a Squalene- and α -Tocopherol-Containing Emulsion for a More Effective SARS-CoV-2 Vaccine. *Pharmaceutics.* 2022 Jul 12;14(7):1455.
33. Bazin HG, Murray TJ, Bowen WS, Mozaffarian A, Fling SP, Bess LS, et al. The ‘Ethereal’ nature of TLR4 agonism and antagonism in the AGP class of lipid A mimetics. *Bioorg Med Chem Lett.* 2008 Oct 15;18(20):5350–4.
34. Drummond RA, Saijo S, Iwakura Y, Brown GD. The role of Syk/CARD9 coupled C-type lectins in antifungal immunity. *Eur J Immunol.* 2011;41(2):276–81.
35. Strasser D, Neumann K, Bergmann H, Marakalala MJ, Guler R, Rojowska A, et al. Syk Kinase-Coupled C-type Lectin Receptors Engage Protein Kinase C- δ to Elicit Card9 Adaptor-Mediated Innate Immunity. *Immunity.* 2012 Jan 27;36(1):32–42.

36. Claassen E, Leeuw W de, Greeve P de, Hendriksen C, Boersma W. Freund's complete adjuvant: an effective but disagreeable formula. *Res Immunol.* 1992 Jan;143(5):478–83.
37. Davidsen J, Rosenkrands I, Christensen D, Vangala A, Kirby D, Perrie Y, et al. Characterization of cationic liposomes based on dimethyldioctadecylammonium and synthetic cord factor from *M. tuberculosis* (trehalose 6,6'-dibehenate)—A novel adjuvant inducing both strong CMI and antibody responses. *Biochim Biophys Acta BBA - Biomembr.* 2005 Dec 10;1718(1):22–31.
38. Abraham S, Juel HB, Bang P, Cheeseman HM, Dohn RB, Cole T, et al. Safety and immunogenicity of the chlamydia vaccine candidate CTH522 adjuvanted with CAF01 liposomes or aluminium hydroxide: a first-in-human, randomised, double-blind, placebo-controlled, phase 1 trial. *Lancet Infect Dis.* 2019 Oct 1;19(10):1091–100.
39. Agger EM, Rosenkrands I, Hansen J, Brahimi K, Vandahl BS, Aagaard C, et al. Cationic Liposomes Formulated with Synthetic Mycobacterial Cordfactor (CAF01): A Versatile Adjuvant for Vaccines with Different Immunological Requirements. *PLoS ONE* [Internet]. 2008 Sep 8 [cited 2020 Apr 27];3(9). Available from: <https://www.ncbi.nlm.nih.gov/pmc/articles/PMC2525815/>
40. Rasheed OK, Ettenger G, Buhl C, Child R, Miller SM, Evans JT, et al. 6,6'-Aryl trehalose analogs as potential Mincle ligands. *Bioorg Med Chem.* 2020 Jul 15;28(14):115564.
41. Smith AJ, Miller SM, Buhl C, Child R, Whitacre M, Schoener R, et al. Species-Specific Structural Requirements of Alpha-Branched Trehalose Diester Mincle Agonists. *Front Immunol.* 2019 Feb 28;10:338.
42. Patin EC, Orr SJ, Schaible UE. Macrophage Inducible C-Type Lectin As a Multifunctional Player in Immunity. *Front Immunol* [Internet]. 2017 [cited 2022 Aug 17];8. Available from: <https://www.frontiersin.org/articles/10.3389/fimmu.2017.00861>
43. Honjoh C, Chihara K, Yoshiki H, Yamauchi S, Takeuchi K, Kato Y, et al. Association of C-Type Lectin Mincle with FcεRIβ Subunits Leads to Functional Activation of RBL-2H3 Cells through Syk. *Sci Rep.* 2017 Apr 10;7(1):46064.
44. Greco SH, Mahmood SK, Vahle A, Ochi A, Batel J, Deutsch M, et al. Mincle suppresses Toll-like receptor 4 activation. *J Leukoc Biol.* 2016 Jul;100(1):185–94.
45. Hao L, Wu Y, Zhang Y, Zhou Z, Lei Q, Ullah N, et al. Combinational PRR Agonists in Liposomal Adjuvant Enhances Immunogenicity and Protective Efficacy in a Tuberculosis Subunit Vaccine. *Front Immunol* [Internet]. 2020 [cited 2022 Aug 17];11. Available from: <https://www.frontiersin.org/articles/10.3389/fimmu.2020.575504>

46. Ma J, Teng X, Wang X, Fan X, Wu Y, Tian M, et al. A Multistage Subunit Vaccine Effectively Protects Mice Against Primary Progressive Tuberculosis, Latency and Reactivation. *EBioMedicine*. 2017 Aug 1;22:143–54.
47. Pahari S, Negi S, Aqdas M, Arnett E, Schlesinger LS, Agrewala JN. Induction of autophagy through CLEC4E in combination with TLR4: an innovative strategy to restrict the survival of *Mycobacterium tuberculosis*. *Autophagy*. 2020 Jun 2;16(6):1021–43.
48. Mohan T, Verma P, Rao DN. Novel adjuvants & delivery vehicles for vaccines development: A road ahead. *Indian J Med Res*. 2013 Nov;138(5):779–95.
49. Wang ZB, Xu J. Better Adjuvants for Better Vaccines: Progress in Adjuvant Delivery Systems, Modifications, and Adjuvant-Antigen Codelivery. *Vaccines*. 2020 Mar 13;8(1):E128.
50. Goodridge HS, Reyes CN, Becker CA, Katsumoto TR, Ma J, Wolf AJ, et al. Activation of the innate immune receptor Dectin-1 upon formation of a 'phagocytic synapse.' *Nature*. 2011 Apr;472(7344):471–5.
51. Johnson DA, Livesay MT. An Efficient Synthesis of 6,6'-DI-O-Acylated α,α -Trehaloses. *J Carbohydr Chem*. 1998 Aug 1;17(6):969–74.